CHALMERS
UNIVERSITY OF TECHNOLOGY

Effect of rheology and crystallinity on processing and barrier properties of PHA

Degree project in Innovative and Sustainable Chemical Engineering

AMIT KUMAR SIVA KUMAR

DEPARTMENT OF INDUSTRIAL AND MATERIALS SCIENCE
CHALMERS UNIVERSITY OF TECHNOLOGY
Gothenburg, Sweden 2023
www.chalmers.se

Master Thesis 2023

Effect of rheology and crystallinity on processing and barrier properties of PHA

AMIT KUMAR SIVA KUMAR

CHALMERS
UNIVERSITY OF TECHNOLOGY

Department of Industrial and Materials Science
Chalmers University of Technology
Gothenburg, Sweden 2023

Effect of rheology and crystallinity on processing and barrier properties of PHA
AMIT KUMAR SIVA KUMAR

Supervisor(s): Ebrahim Shokri, Stora Enso ®
Gisela Cunha, Stora Enso®
Professor Roland Kádár, Chalmers University of Technology®
Examiner: Professor Roland Kádár, Chalmers University of Technology

Master Thesis 2023
Department of Industrial and Materials Science
Chalmers University of Technology
SE-412 96 Gothenburg
Sweden
Telephone +46 31 772 1000

Cover: Carton used on Food service packaging.

Typeset in LaTeX
Gothenburg, Sweden 2023

Abstract

Plastic pollution is one of the major problems that the world is facing at present. Different industrial sectors contribute to this and the packaging sector is one of the main contributors. According to the statistics, the packaging sector alone contributes to 60% of the total plastic pollution. This creates the need for the packaging industry to become more sustainable and produce more environmentally friendly products. There are various types of packaging products and this thesis is focused on food packaging. In food packaging a plastic layer is used to act as a barrier against, for example, gases, such as oxygen and carbon dioxide, and sunlight, as these can decrease the shelf life of the packaged food. However, the plastic film is produced from fossil-based resources and is not biodegradable. The replacement of the conventional plastic barriers with a bio-based polymer is one possible solution to move towards more sustainable packaging materials. For this purpose, a class of bio-based polymers named polyhydroxyalkanoates (PHAs) have been studied in this project. Four different types of PHAs have been characterized using techniques such as DSC, TGA, and DMA, among others. Rheological characteristics were also studied to improve the PHA processing and coating onto paperboard at a pilot scale. Additionally, water vapor barrier properties of the different PHA samples and PHA-coated paperboard were measured and the effect of PHA molecular weight and crystallinity on these was also assessed. From this study, it was observed that PHA with higher molecular weight showed better performance in terms of mechanical properties and barrier properties. Moreover, PHA crystallinity has also been shown to play an important role in terms of barrier properties alongside molecular weight. Regarding rheological properties, it was verified that PHA with higher molecular weight has higher melt viscosity, which makes the material stable at higher temperatures but at the same time, hinders the production of proper coating onto the paper-board. For a better understanding of how PHA processing through extrusion coating can be improved in practice, further studies are required, for instance, the change of processing parameters and the compounding of PHA with other components/polymers.

Keywords: Packaging, polyhydroxyalkanoates, barrier properties, rheological properties, crystallinity, extrusion coating

Acknowledgements

First, I would like to thank my supervisors Ebrahim Shokri, Gisela Cunha and Prof. Roland Kádár for giving me the opportunity to do my thesis under them and for the opportunity to do my thesis at Stora Enso. I had constant support and advice from you and thank you for allowing me to explore freely this topic.

I would also like to thank Mikael Pelcman from Stora Enso and Marko Bek from Rheology and Processing Soft-Matter team at Chalmers for their help during my lab work.

Finally, I would also like to extend my gratitude to the entire team at Stora Enso and the Rheology Processing of the Soft-Matter team at Chalmers for their valuable inputs during my thesis period

Amit Kumar Siva Kumar, Gothenburg, 2023

List of Acronyms

Below is the list of acronyms that have been used throughout this thesis:

PLA	Polylactic acid
PHA	Polyhydroxy alkaonate
PCA	Polycaprolactone
LPB	Liquid packaging board
PE	Polyethylene
SCL	Short chain length
MCL	Medium chain length
P3HB	Poly(3-hydroxybutyrate)
P(3HB-co-3HV)	Poly(3-hydroxybutyrate-co-3hydroxyvalerate)
P(3HB-co-3HH)	Poly(3-hydroxybutyrate-co-3-hydroxyhexonate)
LDPE	Low density polyethylene
CO_2	Carbon dioxide
O_2	Oxygen
N_2	Nitrogen
WVTR	Water vapour transmission rate
OTR	Oxygen transmission rate
T_m	Melting temperature
T_c	Crystallisation temperature
T_g	Glass transition temperature
PET	Polyethylene terephthalate
CH_4	Methane
PHBV	Polyhydroxybutyrate–co-hydroxy valerate
H_2O	Water
HDPE	High density polyethylene
DSC	Differential scanning calorimetry
TGA	Thermogravimetric analysis
DMA	Dynamic mechanical analysis
SEM	Scanning electron microscopy
ICP-OES	Inductively coupled plasma optical emission spectroscopy
FTIR	Fourier transform infrared spectroscopy
PBS	Polybutylene succinate

Nomenclature

Below is the nomenclature of indices, sets, parameters, and variables that have been used throughout this thesis.

M_w	Molecular weight
G"	Loss modulus
G'	Storage modulus
E	Elastic modulus
σ	Tensile stress
ϵ	Tensile strain
τ	Shear stress
L/R	Length/Radius
ΔP	Pressure loss
τ	True (corrected) shear stress
$\dot{\gamma}$	True(corrected) shear rate
τ_a	Apparent shear stress
$\dot{\gamma}_{\mathrm{a}}$	Apparent shear rate
η_{a}	Apparent viscosity
η_{s}	Corrected(true) viscosity
δ	Phase angle

Contents

List of Figures

List of Tables

1

Introduction

1.1 Plastic materials

Conventional plastics are materials made of synthetic polymers. The first fully synthetic plastic was developed in the beginning of 20thcentury. The invention of synthetic plastics made petroleum companies partner up with chemical companies for large-scale production, as their raw material is one of the byproducts of processing crude oil. The first use of synthetic polymer or plastic was during World War II as insulation in radar cables. In the modern world, synthetic plastics are widely used in many industries, including packaging, agriculture, food, consumer products, automobile, medical, and aerospace. The massive and irresponsible consumption of plastics since their industrialization has led to worldwide pollution and other environmental issues, and the packaging sector has been one of the biggest contributors to this. Households contribute to more than 60% of the consumer plastic waste, most of which is single-use plastic that takes decades to decompose[1].

Existing literature on marine litter worldwide shows that plastics contribute to 60-80% of total marine debris. Out of this debris, plastics deriving from packaging materials are one of the most common[3]. The problem with plastics made of synthetic polymers does not stop in marine pollution. In fact, of the total plastics produced worldwide each year, 20% to 25% end up in landfills[4]. This creates a significant strain on municipal budgets for clearing the landfills and following the environmental norms and regulations for discarding plastic waste[1]. The economic burden of moving and recycling plastic waste outweighs that of making new plastic. Thus, more sustainable alternatives are required, and plastics derived from bio-based and biodegradable polymers can be part of the solution.

Bio-based polymers are generally classified into three categories.

- •Polymer produced by chemical synthesis using renewable bio-based monomer.
- •Polymer directly removed from the biomass.
- •Polymer directly produced by microorganisms or genetically modified bacteria

Biodegradable plastics, on the other hand, are defined as polymers that resemble normal plastics but that will break down in nature in the presence of water and microorganisms after being disposed of. Biodegradable plastics can be either bio-based or derived from fossil resources. However, the latter type is less common. Extensive research is being conducted to change the characteristics of polymers so

they can break down more easily into their constituents upon disposal, to minimize their environmental impact[1].

The image below depicts a summary of biodegradable polymer types.

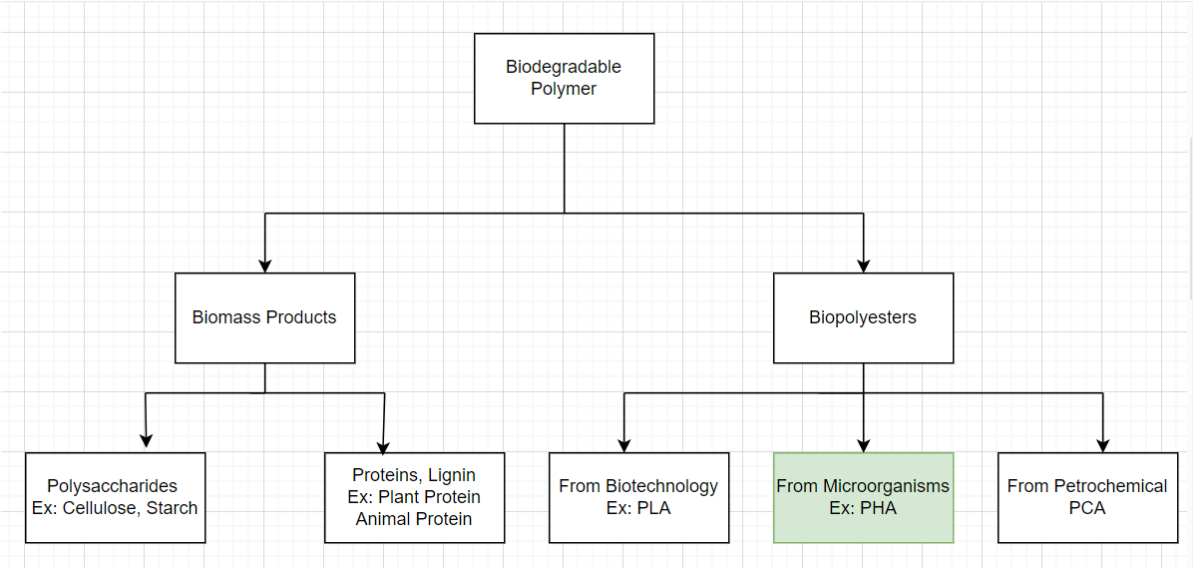

Figure 1.1: Classification of biodegradable polymers[1]

1.2 Bio-based and biodegradable polymers

1.2.1 PLA

PLA is a semicrystalline polymer prepared by polycondensation of lactones or condensation of hydrocarbonic acid[5]. It is biodegradable under composting conditions at elevated temperatures and possesses moderately good mechanical properties [6]. The image below depicts the PLA structure.

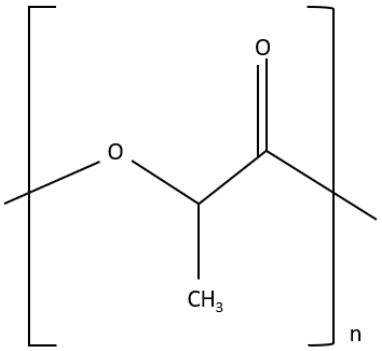

Figure 1.2: PLA structure

Since PLA is bio-based and generally biodegradable, it is currently being widely used in packaging and medical applications[5]. The mechanical, thermal, and rheological properties of the PLA are determined by its Tg temperature. The melt viscosity of the PLA determines the flow conditions and has a significant impact on the processing time[5]. Based on the PLA molecular weight, its processing conditions for extrusion coating on paperboard can vary. For higher molecular weight PLA, the melt viscosity is in the range of 500-100 Pa, and for low molecular weight PLA the polymer melt behaves like a Newtonian fluid(i.e, a fluid that behaves like water)[5]. The crystallinity of PLA is also one of the important factors for the extrusion coating process. PLA with semi-crystalline structure shows higher shear viscosity compared to amorphous PLA within the same processing conditions. The PLA melt also shows a shear thinning behavior with increasing shear rate[5]. Due to the weakening of the interaction of molecular chains at higher shear rates and amplitudes, the shear viscosity also decreases[5]. Thus, the structure and crystallinity of the polymer are important factors affecting the processing conditions.

The thermal properties of the PLA are also determined by its molecular weight and the polymerization conditions [5]. In general, the T_g value of PLA lies in the range 50 - 80°C and T_m in the range 130 - 180°C[5]. The exact value of the T_g and T_m depends on the molecular weight[5].

PLA's mechanical properties vary; it can be either stiff or elastic and soft. PLA is usually compared to PET and it possesses higher tensile strength and tensile modulus than the latter. Its tensile strength is about 59 MPa and the tensile modulus is about 3.8 GPa[5]. PLA also shows superior barrier properties than PET overall. It has better resistance to CO_2, N_2 and CH_2, but low resistance to O_2 compared to PET[5].

1.2.2 PHA

Polyhydroxyalkanoates (PHAs) are a class of naturally occurring bio-based polyesters that are produced by several bacteria[7]. Under certain unbalanced growth conditions, and in the presence of too much carbon, a variety of microorganisms accumulate PHAs as inclusion bodies[8]. PHAs were first discovered in 1926. Since then, they have attracted interest for use in various applications because of their biodegradability, bio-compatibility, and ability to be manufactured from natural carbon sources[9]. PHA polymers backbone is made up of a monomer called R-Hydroxy fatty acid and each monomer contains a saturated alkyl group[10]. However, the side group can also be an unsaturated alkyl group or a branched alkyl group, but the occurrence of the latter is quite uncommon[10]. The image below shows the general structure of PHAs.

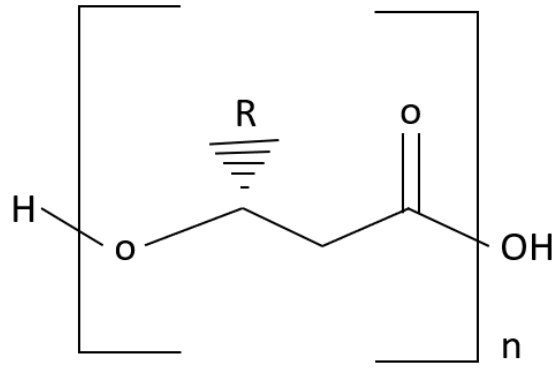

Figure 1.3: General structure of polyhydroxyalkanoates in which R represents $(CH_2)_xCH_3$ moieties

PHAs are generally classified into different types based on the number of carbon atoms in their respective monomers. A short chain length (SCL) PHA contains 3 to 5 carbon atoms and a medium chain length (MCL) PHA contains 6 to 14 carbon atoms[11]. The average molecular weight (M_w) of PHAs is determined by their chain length. In general, the M_w of PHAs is around 50,000-1,000,000 Da and varies with PHA producer[12]. Since their discovery, there are only a few PHA types that have started to be commercialized in recent years. The most common and currently commercialized PHAs are P3HB, (or simple PHB), P(3HB-co-3HV) (or simply PHBV), P(3HB-co-3HH) (or simple PHBH) and P(3HB-co-4HB) (or simply P3HB4HB)[13].

Depending on the grade and structure, PHAs T_m is in the range of 120-180°C and T_g in the range of -20°C to -+15°C. Based on the monomer units present in its structure, PHA can show a wide range of mechanical properties. For instance, a short-chain length (SCL) PHA-like polyhydroxybutyrate (PHB) is considered brittle and has a low impact strength. For co-polymers like poly(hydroxybutyrate-co-hydroxyvalerate) (PHBV), the properties of PHA can be varied by changing the valerate content. The modulus of elasticity of PHA ranges from 0.08GPa to 3.5GPa (very ductile)[5]. The tensile modulus and tensile strength of some PHA are shown in the table below alongside those of LDPE

Table 1.1: Mechanical properties of two of the most common PHAs and LDPE[2]

Polymer type	**Tensile modulus(GPa)**	**Tensile strength(MPa)**
PHB	1.7-3.5	40
PHBV	0.7-2.9	30-38
LDPE	0.2	10-15

The water vapor permeability of PHA is claimed to be of the same level as that of PET. PHAs are highly biodegradable and their degradation can take place both in the presence or absence of enzymes [5]. Even though PHAs possess properties comparable to those of fossil-based polymers, one of the main disadvantages of PHAs

is the fact that the difference between their processing temperature and thermal degradation temperature is too low, which makes it difficult to properly process the material without triggering thermal decomposition.

1.2.3 Other biopolymers

The growing demand for sustainable materials has brought much attention to cellulose. Cellulose is a polysaccharide and the most abundant naturally occurring biodegradable polymer on earth[5]. The image below depicts the cellulose structure.

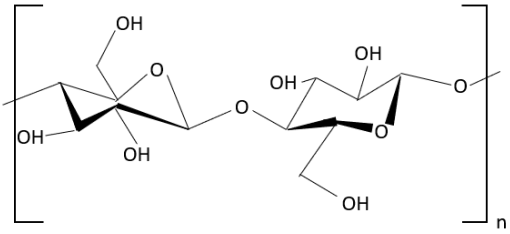

Figure 1.4: Cellulose structure

The hydroxyl groups in cellulose structure allow the formation of a vast hydrogen bonding network, which makes cellulose strong and insoluble in most of the solvents, including water[5]. Despite being insoluble in water, cellulose is highly hydrophilic and can absorb high amounts of water and swell. Cellulosic materials have in general very good mechanical properties but have usually high permeability to air and water[5]. To compensate for the poor barrier performance, cellulose is generally combined with other synthetic materials.

Starch is another abundant polysaccharide like cellulose and its characteristics are also studied for usage as a bio-based barrier in packaging materials. The structure of the starch is shown below.

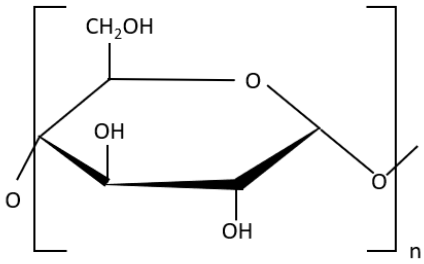

Figure 1.5: Starch structure

Starch has two main components, amylose and amylopectin. It has generally low stability under stress and its amylose component is soluble in water[5]. In terms of mechanical properties, these can greatly vary due to the big variation of molar

masses of amylose and amylopectin. Like cellulose, starch is also biodegradable and, due to this, it is typically used as a natural filler in polyolefins, such as high-density polyethylene (HDPE).

1.3 Packaging material

Bio-based and biodegradable polymers for packaging materials have drawn increasing attention globally. As mentioned earlier, the use of bio-based polymers can greatly decrease toxicity and increase the chances of biodegradability and sustainability of end products. In addition, the carbon footprint can also be reduced[14].

One of the main components of fiber-based packaging materials is paperboard. Paperboard provides the necessary mechanical support but needs additional components to enhance the barrier performance of the packaging material. The barrier properties, such as against odor, moisture, grease, oxygen, and water[14], are typically improved by coating the paper board on both sides with synthetic polymers. As mentioned above, since the invention of packaging materials, fossil-based polymers have been widely used as barrier coating due to their easy processability and relatively low price.

Plastic waste (19.4%) is the second most common waste after paper and cardboard (40.6%) within packaging materials. Packaging waste reached 178 kg per capita in 2019 and it has been reported that Ireland is at the top of the members in the European Union when it comes to packaging waste, while Sweden is in 22nd place[14]. Though Sweden is almost at the bottom, efforts are still being taken to further reduce the environmental impact. Stora Enso, the renewable materials company, is making efforts from its side to minimize waste production and its impact.

1.3.1 Packaging demands

1.3.1.1 Packaging systems and types

Food packaging technology is constantly improving in response to modern society's expanding challenges and requirements[15]. The packaging industry employs a diverse range of materials and printing processes to create packages that look attractive and help us keep the packaged product safe[6]. Packaging systems also play a crucial role in marketing by providing an opportunity to differentiate the products and make them more attractive. In general packaging systems can be divided into three types.

• Primary packaging: These are the packaging types that come in direct contact with the food. Some examples of primary packaging are laminated pouches, plastic containers, C arton packages, etc.

• Secondary packaging: This type of packaging usually holds together individual units of goods. Some examples of secondary packaging are plastic crates, plastic

trays, etc.

• Tertiary packaging: This type of packaging deals with the type of packaging used to transport for example large quantities of wood from one place to another. Some examples are wooden containers, wooden pallets, etc.

The primary packaging system is important because it comprises food packaging. Within the primary packaging, usually a barrier material protects the food from carbon dioxide, oxygen, and water vapor, among others. There are various types of materials that can be used as barriers. Some of the most used barrier materials are metals, glass, plastic, and laminates. Among these packaging materials, LDPE plastic, as mentioned above is the most widely used in today's scenario.

1.3.1.2 Packaging properties

When it comes to packaging materials, various demands arise throughout the entire value chain of the product. Most of the properties are associated with the polymer used. The properties of importance can be divided into three main categories
• Barrier properties
• Stiffness(i.e.,mechanical properties)
• Sealing properties

1.3.1.3 Barrier properties

In a fiber-based packaging context, a barrier is a layer of material that is coated or laminated onto paperboard to prevent the migration of unwanted substances like water, into the packaging, thus increasing the shelf-life of the food product. The migration of oxygen must also be prevented, as it can change the nutritional value of the product. The barrier material must also hinder the penetration of light, as it can induce chemical processes, such as photo-oxidation, vitamin loss of the food product, etc.

The barrier properties are usually tested with three main types of experiments.
• Water Vapour Transmission Rate(WVTR) test to assess water vapour barrier performance
• Oxygen Transmission Rate(OTR) test to assess Oxygen barrier performance
• Grease barrier test to assess grease barrier performance.

1.3.1.3.1 WVTR test The WVTR test is a standard test (ASTM F1249-20) that measures how much water vapor can transit through the thickness of the packaging material. The instrument measures the weight increase of the material over the period of the experiment. The test can be done at different temperatures and relative humidity conditions, but most commonly is done at i) normal conditions – 23°C and RH=50% and/or ii) tropical conditions – 38°C and RH=80%.

1.3.1.3.2 OTR test The OTR test (ASTM D3985-17) is done to measure how much oxygen can transit through the thickness of the packaging material. It is one of the important tests as oxygen can change the nutritional value and odour of the food product. In this test, the packaging material sample is usually placed in a chamber, and oxygen is allowed to pass through it. A sensor placed inside the instrument measures the amount of oxygen that is passed in a fixed interval of time and the test is complete when the amount that passes through the film becomes constant.

1.3.1.3.3 Grease barrier test Grease barrier is also one of the important tests that are measured on polymer-coated paperboard. There are different ways to assess oil and grease barrier properties. One way is to test how much time it takes for oily or greasy substances used in food to penetrate through the coated paperboard, for example, mayonnaise, chicken fat, etc. Another way is to use the KIT method and test if twelve liquid solutions with different polarities can penetrate the coated paperboard. The highest numbered solution that remains on the surface of the paperboard without causing failure is reported as the 'kit rating' (maximum 12).

1.3.1.4 Stiffness(mechanical properties)

Stiffness provides information about the behavior of a material when an external force is applied, i.e., it tells the extent to which it can resist deformation in response to that force. Stiffness is one of the important properties because, from the preparation of the packaging material to the end use of the package, the material is subjected to different types of forces and bending. So, the packaging material must have the capacity to be bent and withstand different forces during converting. To assess the stiffness of the material, Elastic Modulus can be determined through tensile testing, and/or bending resistance can be analyzed.

1.3.1.5 Sealing properties

Selability and seal strength are also important parameters of a packaging material. A packaging material should have good sealing so that the packaged content doesn't get leaked through the seal. Depending on the structure of the packaging material, different sealing techniques can be used, namely: heat sealing, cold sealing, and ultrasonic sealing. In the case of a heat-sealed material, the sealing strength is measured by first heat-sealing the packaging material sample at a particular temperature, pressure, and time, and then measuring the force required to break apart the seal, which is done by pulling away the material near the seal area using a tensile tester.

1.3.2 Liquid packaging board structure

Liquid packaging board (LPB) has been used for the production of food containers for liquids and creamy substances for more than 40 years. It is used to protect and transport food, and to avoid its contamination by external sources. A typical

structure of aseptic LPB is shown in Figure1.6

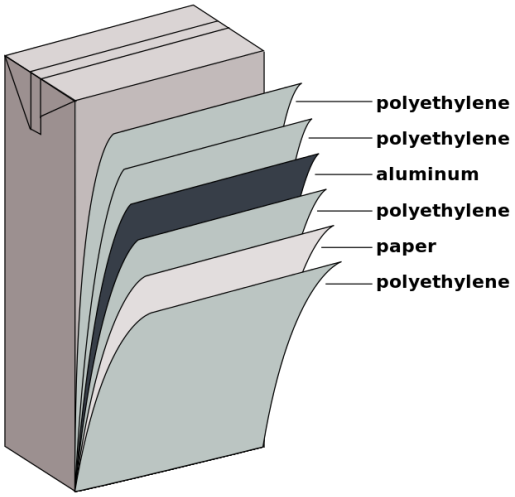

Figure 1.6: LPB structure

The above picture depicts the different layers present in an aseptic LPB, meaning an LPB that requires a long shelf-life, even at ambient conditions. In order to protect the food, four layers are typically present on the inner side of the paperboard (i.e., towards the packaged product), and one of the plastic layers is the one in contact with the food. The outer side of the paperboard is known as the printing surface, on which information about the product and brand are printed. On the top of the printing surface another plastic layer is added, typically named the condensation layer. Today most of the plastic laminates used in LPB contain low-density polyethylene (LDPE). Depending on the application of the LPB, the number of layers can vary. While typical aseptic LPB contains both LDPE and aluminum layers, LPB for shorter shelf-life applications contains only LDPE. Being LDPE derived from fossil-based resources and not biodegradable, to produce more sustainable packaging materials, and in specific LPB, one needs to focus on the replacement of LDPE by other more sustainable alternatives. In this project polyhydroxyalkanoates (PHA) were chosen for this purpose.

1.4 Extrusion coating

Extrusion coating is one of the first processes designed to extrude thermoplastic polymers onto flexible substrates. Since its introduction, extrusion coating has been continuously developed over the years and nowadays it turned into one of the most used processes for extrusion and lamination of plastics [16].

The first extrusion coating was done with polyethylene on the paperboard. Since then it has been used for the extrusion of different polymers and for various applications. In extrusion coating a thin film of hot molten polymer comes out the of extruder and is passed to a cooled nip reel assembly (Figure1.7A). The length and thickness of the extruded film are determined by the type of die utilized. Typically,

the extrusion coating of a polymer film on a paperboard leads to a coat weight in the range of 10-75 g/m2. The part of the equipment that coats the polymer film onto the paperboard is also sometimes called a laminator[16]. The molten polymer that comes out of the die is pulled towards the nip, which is formed by a chill roll and a rubber pressure roll. The substrate (e.g., paperboard) is fed continuously and it is pressed with the polymer melt. Due to the compression force applied by the pressure roll, the polymer melt gets adhered to the substrate[16].

The position of the chill roll with respect to the die is of critical importance. The melt entry angle and height from which the chill roll is placed (air gap) also determine how well the polymer can be coated on the paperboard. The polymer melt must be fluid enough to flow onto the surface of the substrate continuously and it is cooled immediately so bonds get formed with the substrate. The thickness of the coated film on the substrate depends on the relative velocity of the extruder to the chill roll. The pressure roll is associated with a backup roll that removes the heat from the former while being cooled with water at a temperature in the range of 15-20°C [16]. The image below demonstrates the extrusion process.

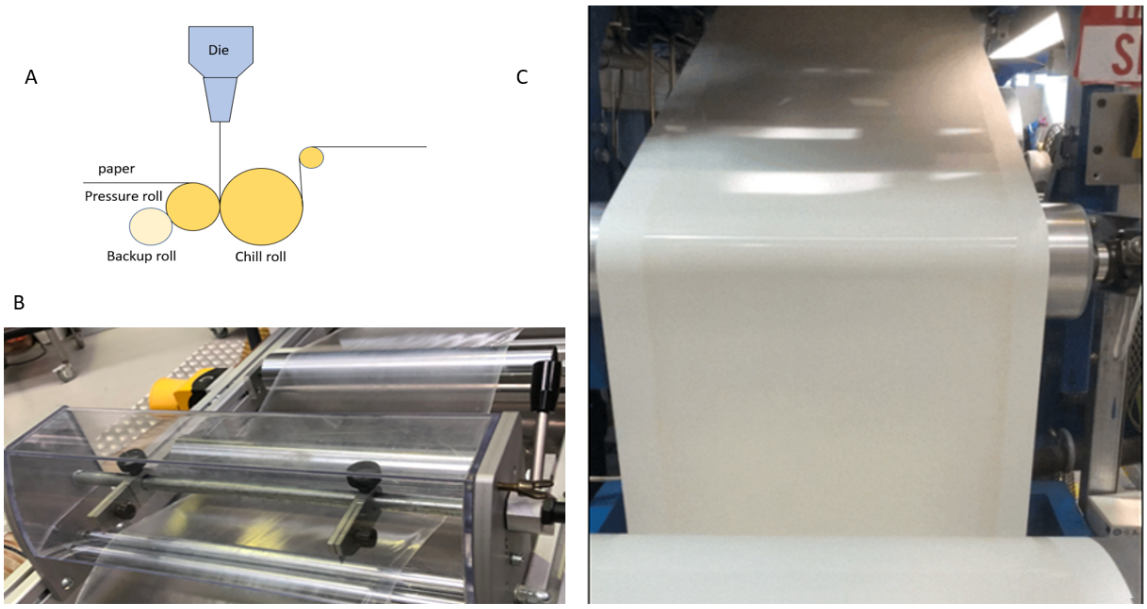

Figure 1.7: A. Shows the typical cross-section scheme of the most important parts of the extrusion process; B. Extrusion of PHA film at pilot scale; C. Extrusion-coated paperboard at pilot scale

1.5 Objectives

The main objectives of this Master thesis project were
• To characterize different PHA samples in terms of properties relevant to their processing within extrusion coating: melting temperature, glass transition temperature, crystallinity, thermal stability, and rheological properties of the polymer melt.

• To evaluate some of the properties of the produced PHA-based materials relevant for packaging materials: heat seal strength, mechanical and water vapor barrier properties.
• To understand how the rheological properties of PHA may affect the extrusion coating process.
• To assess how PHA crystallinity may affect barrier properties of ensuing materials.
• For this purpose, both hot-pressed PHA films, prepared in-house, and PHA-coated paperboard, produced at pilot scale, were analyzed.

1.6 Limitations

In this thesis only technical properties of different PHA types and samples prepared thereof were assessed. Other aspects that are usually of interest when a new polymer is to be introduced into the packaging world, such as feedstock, geographical availability, and cost, were not in focus. Moreover, due to time constraints, normal for a Master thesis project, the type of characterization to be done on the PHA samples was limited to a number of prioritized parameters, and some other relevant properties were not assessed, for instance, recyclability and compostability/biodegradability of the PHA-based materials.

There were also some technical constraints worth mentioning: i) since no extruder was available in-house, PHA films were produced at lab-scale with a hot-press instead; ii) since technical issues (i.e., related to PHA stickiness) were encountered when trying to analyze M_w of the PHA samples using Gel Permeation Chromatography (GPC), one needed to rely on M_w information present on the technical data sheet of the material.

2
Materials and Methods

2.1 Materials

Four different PHA types in granulate form were studies. The four PHA types will be termed throughout the thesis as PHA A, PHA B, PHA C, and PHA D. In the table below, information obtained from the respective technical data sheets regarding the molecular weight of the four PHA types is listed. Along with these PHA and LDPE coated paper board were obtained from the pilot trials and the average thickness of the samples was 280μm.

Table 2.1: Qualitive molecular weight of the different PHAs studied

Material type	**Molecular weight**
PHA A	Low molecular weight
PHA B	Medium molecular weight
PHA C	High molecular weight
PHA D	High molecular weight(blend with PBS)

2.2 Experimental methods

2.2.1 Film preparation

Films of all four PHA types and also LDPE (reference) with an average thickness of 45μm were produced in-house by compression moulding using a Collin hot-press. Prior to hot-pressing, the granulates (except LDPE) were dried at 60°C for 4 hours to remove any residual water that could evaporate and originate bubbles during hot-pressing. The hot-press was set to 175°C (120°C for LDPE) and the mould setup (Figure2.1) was pre-heated at this temperature. Release films were placed on metal plates and the metal frame was placed on the bottom metal plate. The metal frame dimensions were 14 cm x 14cm with a thickness of 0.1 mm. The polymer granulates were placed in the center of the frame and the top metal plate was brought down into contact with the bottom metal frame to melt the granulates without any additional pressure. The granulates were left to melt for 14 min and then a pressure of 100 bar was applied for 2 min. After pressing, the mould setup was taken out and left to

cool down for 3 minutes. Then the polymer films were carefully removed from the release films. The table below summarizes the conditions used to prepare the films.

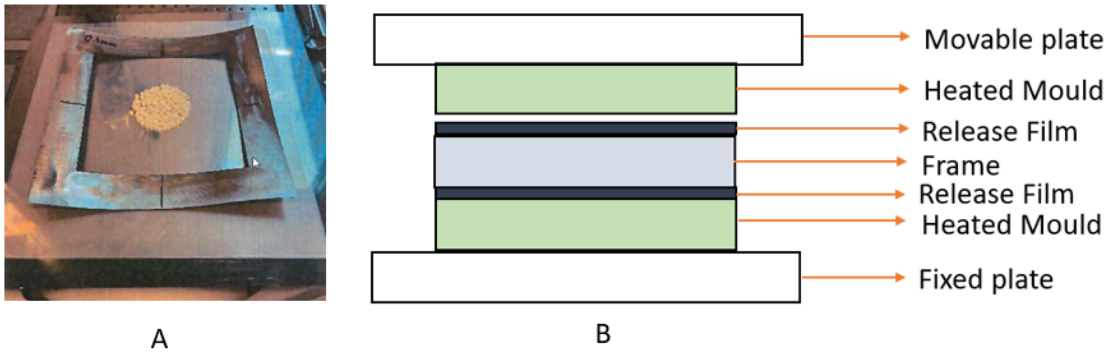

Figure 2.1: A.Sample pack setup in hot press B.Schematic representation of the setup

Table 2.2: Summary of the conditions used to prepare PHA and LDPE films with hot-press

Material type	**Pre heating temperature (°C)**	**Preheating timing (h)**	**Melting temperature (°C)**	**Melting time (min)**	**Pressure applied (bar)**	**Pressure applied timing (min)**
PHA A	60	4	175	14	100	2
PHA B	60	4	175	14	100	2
PHA C	60	4	175	14	100	2
PHA D	60	4	175	14	100	2
LDPE	no preheating	-	120	14	100	2

2.2.2 Differential Scanning Calorimetry(DSC)

DSC is a thermal analysis technique that can provide various polymer characteristics, such as melting temperature, glass transition temperature, crystallization temperature, enthalpy of fusion, etc., by measuring the difference in the amount of heat required to increase the temperature of a polymer sample and reference as a function of temperature. The reference sample(Platinum crucible pan), is also exposed to the same conditions as polymer sample[17].

DSC measurements were done using a TA Instruments Q2000 device. Four heating and cooling cycles were measured. In the heating cycles, 10mg polymer samples were first equilibrated at -20°C for 5 min and then heated to 190°C with a heating

rate of 20°C/min. In the cooling cycles, the samples were then kept at 190°C for 2 min before being cooled down to -20°C at the same rate used for heating. Nitrogen was used as purging gas and the flow rate was kept at 50 ml/min. For all PHA samples, the first cycle was disregarded for further calculations since it is usually associated with the polymer's thermal history.

Alongside with the T_m and T_c, the crystallinity (in percentage) was also calculated from the DSC curves for the different PHA's. Crystallinity for each PHA sample was calculated based on the ratio between its melting enthalpy and that of a 100% crystalline PHA polymer, which was obtained from the literature. The same procedure was followed for analyzing PBS.

2.2.3 Thermogravimetric Analysis(TGA)

TGA analysis is a technique in which the polymer sample is subjected to a defined temperature program. In this analysis, the temperature is raised at a constant rate and the mass of the material is recorded with the rise in temperature[18]. TGA provides a good insight into the thermal stability of the material since it enables to assess at what temperature the material starts degrading (thermal degradation).

TGA analysis was done using a TA Instruments Q5500 device. The samples were first equilibrated at 40°C and then heated to 105°C with a heating rate of 5°C/min. Then the samples were kept isothermal for 20 min and then again heated to 700°C with a heating rate of 5°C/min. At 700°C the samples were also kept isothermal for 20 min. The obtained thermograms depict the mass change with respect to the increasing temperature. Air was used as purging gas with a flow rate of 10 ml/min.

2.2.4 Dynamic Mechanical Analysis(DMA)

DMA is used to investigate the molecular relaxation in polymers and to calculate inherent mechanical and flow properties as a function of time and temperature. DMA can be used to find in an accurate way the glass transition temperature (T_g) of a polymer. In DMA, the storage modulus (G') and the loss modulus (G") of the material is measured while ramping the temperature at a constant amplitude. With the value of G' and G", one can determine $\tan(\delta)$. Then, the T_g is obtained as the peak value in the Temperature vs $\tan(\delta)$ graph[19]

DMA evaluation was done with an Anton Paar MCR702 Twindrive rotational rheometer. The analysis was carried out at the temperature range of -40°C to +40°C. First, the strain sweep test was done to determine the linear viscoelastic region. From the strain sweep test, the strain of 0.008% was selected. The dimensions of the films used for the testing were 12mm x 20mm. Once the sample was mounted the temperature was decreased to -40°C at a cooling rate of 8°C/min. A constant normal force of -0.04N was applied to keep the sample in tension as the films were thin. Then, at the constant strain of 6 rad/s, the temperature was raised to +40°C at the heating rate of 2°C/min. The data was recorded and the temperature was brought

back again to room temperature before the next sample was loaded.

2.2.5 Fourier Transform Infrared Spectroscopy(FTIR)

FTIR is one of the analysis techniques used to characterize the chemical composition of polymeric materials. In this project, FTIR was performed using a Bruker Platinum device coupled with an ATR cell. The analysis was done with an accumulation of 24 scans and the resolution of 1cm^{-1} was used to record the spectra.

2.2.6 Mechanical Properties

The mechanical properties of interest in this project were tensile strength, tensile or Elastic modulus, and heat seal strength.

2.2.6.1 Tensile testing

The tensile modulus, also known as elastic modulus or Young's modulus, gives information about the linear elasticity of the material. The elasticity of the material is evaluated based on the relationship between deformation and the force or power required for this deformation to happen. Young's modulus is given by the equation:

$$E = \sigma/\epsilon \tag{2.1}$$

E = Elastic modulus
σ = Stress
ϵ = Strain

The maximum stress and the elongation a material can handle before it breaks can be measured during tensile testing. The tensile testing was performed using a Zwick/Roell machine equipped with a 100 N load cell. For every experiment, a preload of 0.2 N was applied to keep the film in tension as the films were thin. The films used for the experiment were cut into dumbbell shapes of 30mm x 5mm using a die cutter with the right dimensions (see Figure2.2) and the test was performed at a speed of 50 mm/min as per ISO standard. For each PHA type, 10 replicates were analyzed and the average values were then calculated.

2.2.6.2 Seal strength testing

One of the important requirements for a packaging material is its sealability and seal strength. The heat sealing test was performed by first using a Param HST-H3 heat sealer device to seal the polymer films and subsequently, the force required to break the sealing, meaning the seal strength, was then evaluated using an Instron 5969 tensile tester. The hot-pressed films were cut into dimensions of 60mm x 15mm. Then two samples of the same type of PHA film were pressed together at the top (see Figure2.2) under a specific sealing temperature with a dwell time of 1 second and pressure of 200 kPa. The heat sealing was performed at six different temperatures: 175°C, 180°C, 185°C, 190°C, 195°C and 200°C. Then, as mentioned above, the seal strength of the samples was tested using a tensile testing machine by clamping the

lower ends of both films to one of the two clamps. A 500 N sensor was used as a load cell and a pre-load of 4 N was applied to keep the sample under tension. The test was performed at the speed of 50 mm/min and the force required to break the seal was recorded. This test was performed on 5 replicates for each PHA type and for each temperature, and then average values were calculated.

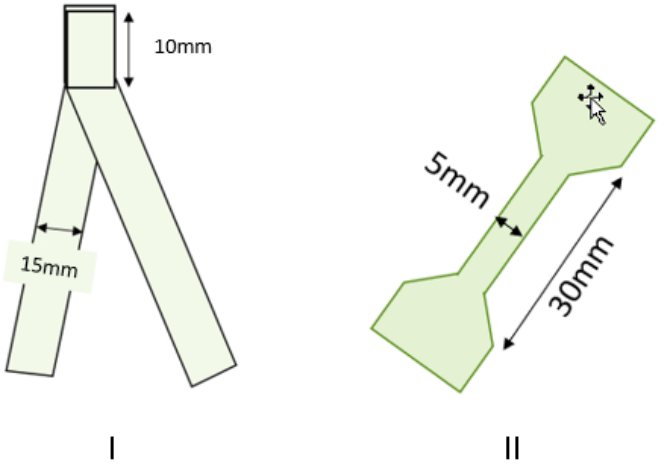

Figure 2.2: Sample structure used for I. Seal strength testing(ISO 11607); II. Tensile testing(ISO 527-1)

2.2.7 Rheological properties

Rheology refers to the study of matter when subjected to flow or deformation. Rheological measurements can provide information on how to achieve a uniform coating of a certain polymer on paperboard without defects. Some of the defects that can be avoided are bubbles, streaks, edge defects, etc.

2.2.7.1 Rotational rheometry

Rotational rheometry measurements were done using an Anton Paar MCR702 TwinDrive instrument. The rotational rheometer was used to study the thermal stability of the material, together with strain sweep and frequency sweep tests. The rheometer was equipped with a convection oven CTD450. A cone-plate measuring geometry having 2° angle and 25 mm diameter and the bottom with a flat plate of 30mm diameter was used. For each test, the oven was pre-heated to the desired temperature and then the polymer granulates were loaded. The distance between the top and bottom plate was 0.106 mm (standard for the measuring geometry used). The table below summarizes the measurement conditions used for the different rheological tests.

Table 2.3: Rotational rheometer measurement conditions

Test type	**Amplitude-Strain(%)**	**Frequency(Hz)**	**Temperature(°C)**
Thermal stability	0.05	1	175 and 160
Strain Sweep test	1 to 1000	1	160
Frequency Sweep test	1	0.01 to 100	160

2.2.7.2 Capillary rheometry

A Göttfert RG20 capillary rheometer was used to measure the melt viscosity at processing-relevant shear rates. After setting the test temperature, the cylindrical barrel of 15 mm diameter was filled with polymer pellet which were let to melt down for 10 min. Then the piston was lowered to the measuring position. The rheometer measures the shear rate and shear stress based on the value of pressure, piston speed, and capillary die used. The pressure measurement is done above the capillary die in the barrel, hence a correction factor was applied to get the actual shear stress. The basic rheological properties in capillary rheometry are determined based on Newtonian fluid assumption, thus a shear rate correction was also applied to get the true shear rate. Once the true shear rate and shear stress were estimated, the true melt viscosity (η) was calculated. The image below depicts the cross-sectional view of the capillary rheometer.

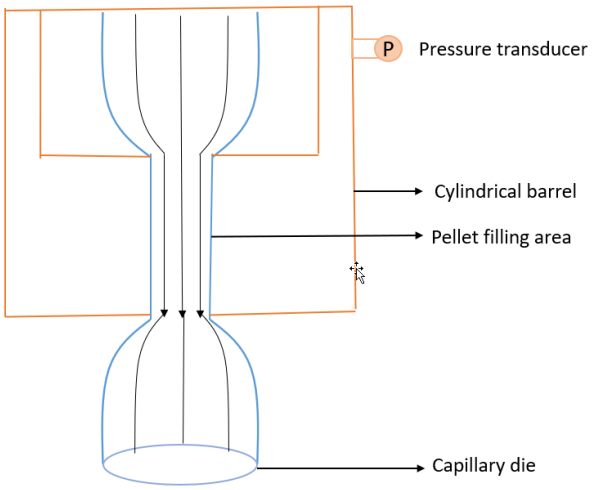

Figure 2.3: Cross-sectional view of a capillary rheometer

BAGLEY CORRECTION

The Bagley correction is used for shear stress correction. At first, a capillary die of diameter 1 mm and length 20 mm is used and apparent values of shear rate and shear stress are measured. Then the capillary die is changed to that of a diameter

of 1 mm and length of 0.2 mm and the shear rate and shear stress are measured again. The true shear stress is calculated as follows

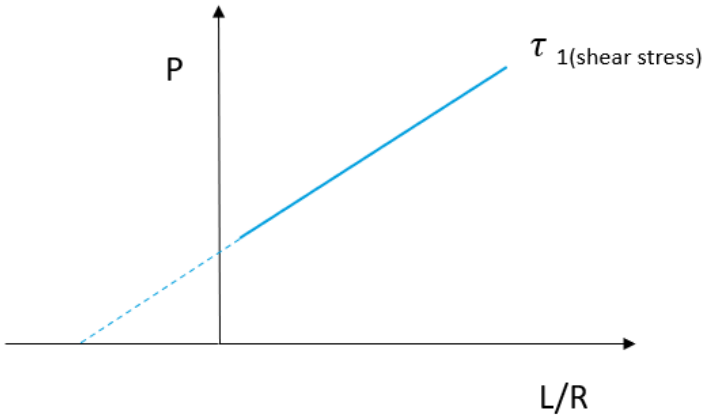

Figure 2.4: Bagley correction graph

$$\tau = (\Delta P)/2 * (L/R + e) \tag{2.2}$$

ΔP = Pressure difference between inlet and outlet
L/R = length by radius ratio of capillary dies
e = Indicates the extrapolated value to x axis

For a given shear rate, pressure values as well as their corresponding L/R ratio are taken from both capillary dies. The values are plotted with pressure at the y-axis and L/R ratio at the x-axis, this gives a two-point straight line. This line is extrapolated to the x-axis which gives e value. These values are substituted in the formula above to get true shear stress (τ). Corrected shear stress values were calculated for every shear rate using the steps described.

WEISSENBERG-RABINOWITSCH CORRECTION
The different polymer melts showed shear thinning flow behaviour. Due to this, shear rates ($\dot{\gamma}$) at the wall are high, but the instruments assume a Newtonian flow behaviour (see Figure2.5) and only measure the apparent shear rates. Hence, a correction factor must be introduced to get corrected true shear rates.

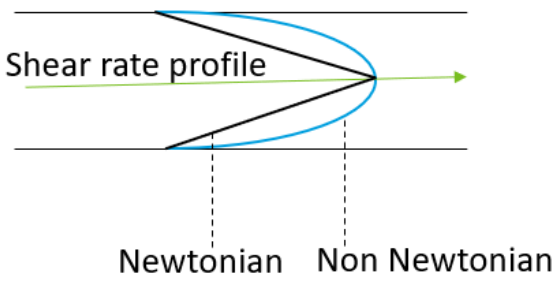

Figure 2.5: Shear rate profile

The shear rate was corrected using the formula below

$$\dot{\gamma} = ((3 * n + 1)/(4 * n)) * \dot{\gamma}_{\mathrm{a}} \tag{2.3}$$

To find the value of n the power law model was used

$$\tau_{\mathrm{a}} = K * {\dot{\gamma}_{\mathrm{a}}}^{n} \tag{2.4}$$

τ_{a} = shear stress apparent
K = flow index
$\dot{\gamma}_{\mathrm{a}}$ = apparent shear rate

Taking logs on both sides gives

$$\log(\tau) = n * \log(\dot{\gamma}_{\mathrm{a}}) + \log(k) \tag{2.5}$$

This equation is of the form $Y = Mx + C$ where C represents the interception and M represents the slope,here n represents the slope and $\log(k)$ represents the y-interception. These equations are applied for every shear rate to get true shear rates

Once the true shear rate and stress are obtained the true melt viscosity(η_{s}) is calculated using the formula below.

$$\eta_{\mathrm{s}} = \tau/\dot{\gamma} \tag{2.6}$$

2.2.8 Water Vapour Transmission Rate(WVTR)

Water vapour transmission rate (WVTR) analysis was done to assess the barrier performance of both the hot-pressed PHA films and PHA-coated paperboards against moisture. The analysis was done using a ProUmid dynamic vapour sorption analyzer. The samples were cut into round shapes of a diameter of 7 cm possessing six small holes in the circumference for screwing the samples onto the chamber. In each chamber, 5 grams of molecular sieves were placed so that the bottom was fully covered. The samples were then placed and screwed onto the chamber. The barrier properties were assessed under two different environmental conditions: normal conditions - 50% relative humidity and temperature of 23°C and tropical conditions - 80% relative humidity and temperature of 38°C.

3

Results and Discussion

3.1 DSC

The DSC measurements were carried out to get more information about the different PHA types studied in this project and find, among other things, their melting temperature, which can give a good understanding of the optimal operating temperature for the extrusion coating process. The image below shows an example of the DSC curves obtained in the different heating and cooling cycles for PHA A and PHA D (the DSC curves for the other PHA types can be found in the appendixA.1 and A.2)

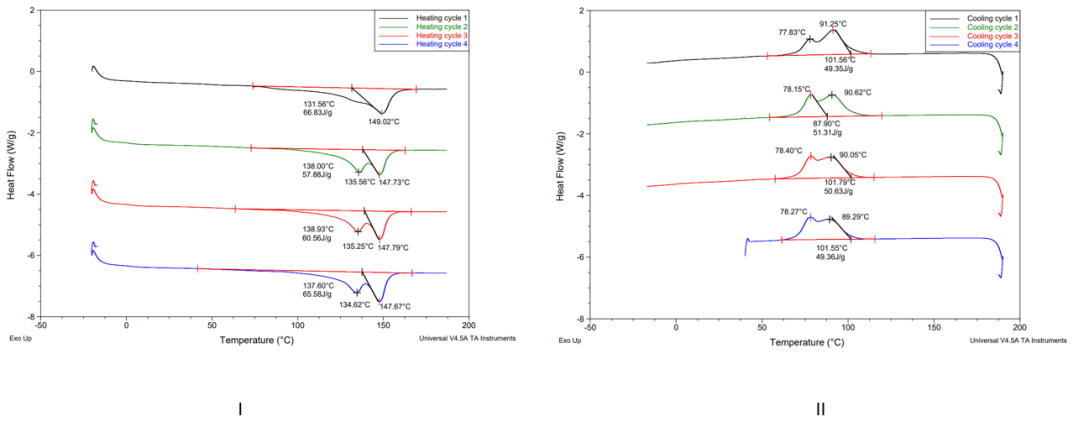

I II

(a) PHA A

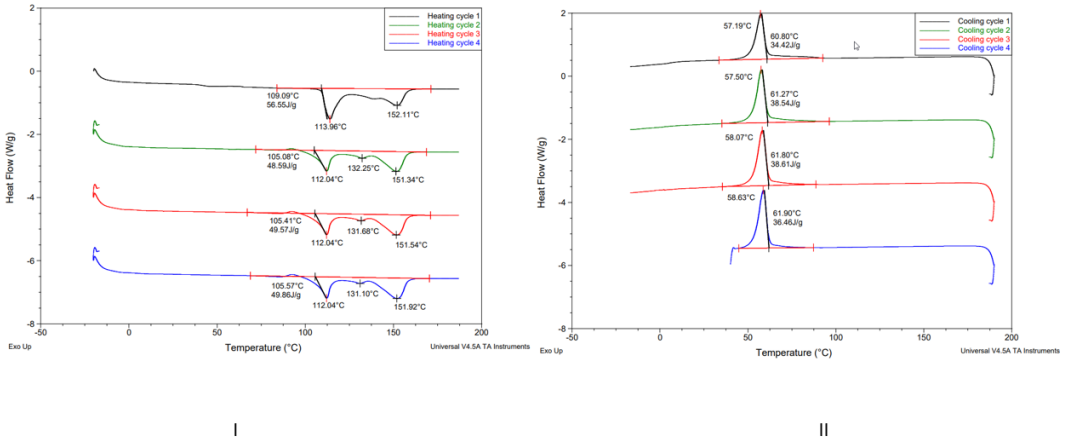

I II

(b) PHA D

Figure 3.1: DSC curves obtained in different (I)heating and (II)cooling cycles

From the image above, it is possible to observe that there are two endothermic peaks in the heating curves of PHA A (Figure:3.1 (a)-I) and three endothermic peaks in those of PHA D (Figure:3.1 (b)-I). For the other PHA types, only 2 endothermic peaks were observed as in the case of PHA A (FiguresA.1 and A.2). The presence of two endothermic peaks indicates that PHA A, PHA B, and PHA C contain two different polymers that melt at different temperatures, which is in tune with the information in the technical data sheet. In the case of PHA D, which was known from the beginning to be a blend with PBS, apart from the two peaks corresponding to two different polymers (also in tune with the information in the technical data sheets), its DSC heating curves also showed a third peak likely assigned to PBS. To corroborate that PBS was really present in PHA D, DSC measurement was also carried out for pure PBS. The DSC results for PBS(Figure:3.2) showed that its melting temperature is around 114°C, which is in tune with the temperature at which the third peak appears in the heating curves of PHA D.

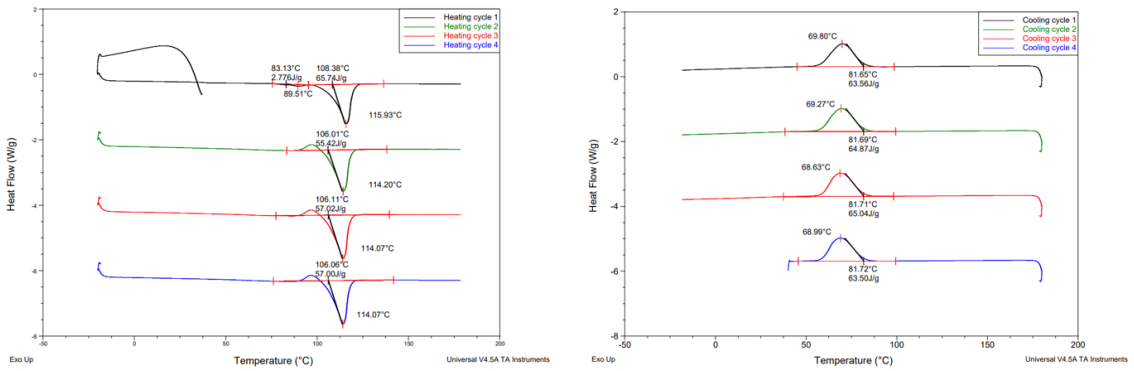

I II

Figure 3.2: DSC curves of PBS obtained in different heating(I) and cooling(II) cycles

PHA A and PHA C also showed two exothermic peaks during the crystallization process, which indicated that the two constituent polymers don't co-crystallize at the same temperature.

The table below summarizes the average values of T_m,T_c and T_g of the different PHAs studied and of LDPE. The melting enthalpy of PHA D alone was calculated by integrating two peaks of PHA and neglecting the PBS associated peak.

Table 3.1: DSC results for the PHAs studied and LDPE

Material type	**Average melting temperature (°C)**	**Average crystallisation temperature (°C)**	**Average melting enthalpy (J/g)**
PHA A	T_{m1} = 135.1, T_{m2} = 147.7	78.3	61.3
PHA B	T_{m1} = 128.1, T_{m2} = 144.6	70.6	59.2
PHA C	T_{m1} = 136.0, T_{m2} = 153.3	68.0	42.1
PHA D	T_{m1} = 131.7, T_{m2} = 151.6, T_{m3} = 114.1	58.1	25.1
LDPE	T_{m1} = 107.2	95.4	127.2

As could be expected, there seems to be a certain correlation between Tm and Mw; PHA samples with the lowest Mw (PHA A and PHA B) generally presented the lowest Tm values, while PHA samples with the highest M_w (PHA C and PHA D) presented the highest Tm values.

Based on the melting enthalpy values, the crystallinity of each PHA type was calculated. The melting enthalpy of a 100% crystalline polymer(146 J/g) was taken from the literature [20]. The crystallinity was also calculated for LDPE (the reference sample) taking into account its melting enthalpy value. The melting enthalpy of 100% crystalline LDPE(293J/g) was also taken from the literature[21]. The table below summarizes the crystallinity for the different PHA types and LDPE

Table 3.2: Percentage of crystallinity for the different PHAs studied and LDPE

Material type	**Average melting enthalpy of sample (J/g)**	**Melting enthalpy of 100% crystalline polymer(J/g)**	**Crystallinity(%)**
PHA A	61.3	146	41
PHA B	59.2	146	40
PHA C	42.1	146	29
PHA D	25.1	146	17
LDPE	127.2	293	43

PHA and PHA B seem to have similar crystallinity to that of LDPE, PHA C and PHA D have significantly lower crystallinity, being PHA D apparently the least crystalline material. The blending with PBS may have contributed to this low crystallinity[22]. The crystallinity values are also used in the section below to try to identify the impact of crystallinity on the water vapor barrier properties of the different PHA samples. In general, it is believed that by increasing the crystallinity

of a polymer, its WVTR should decrease. Nonetheless, it is worth noting that several other factors also have an effect, such as the molecular weight and degree of polymerization of the polymer, the quality of the coated film *etc.*

3.2 TGA

The TGA analysis can provide useful information about the maximum recommendable temperature to process PHA during extrusion coating. The thermograms of the different PHA types and LDPE in the image below show how their mass is affected by increasing temperature.

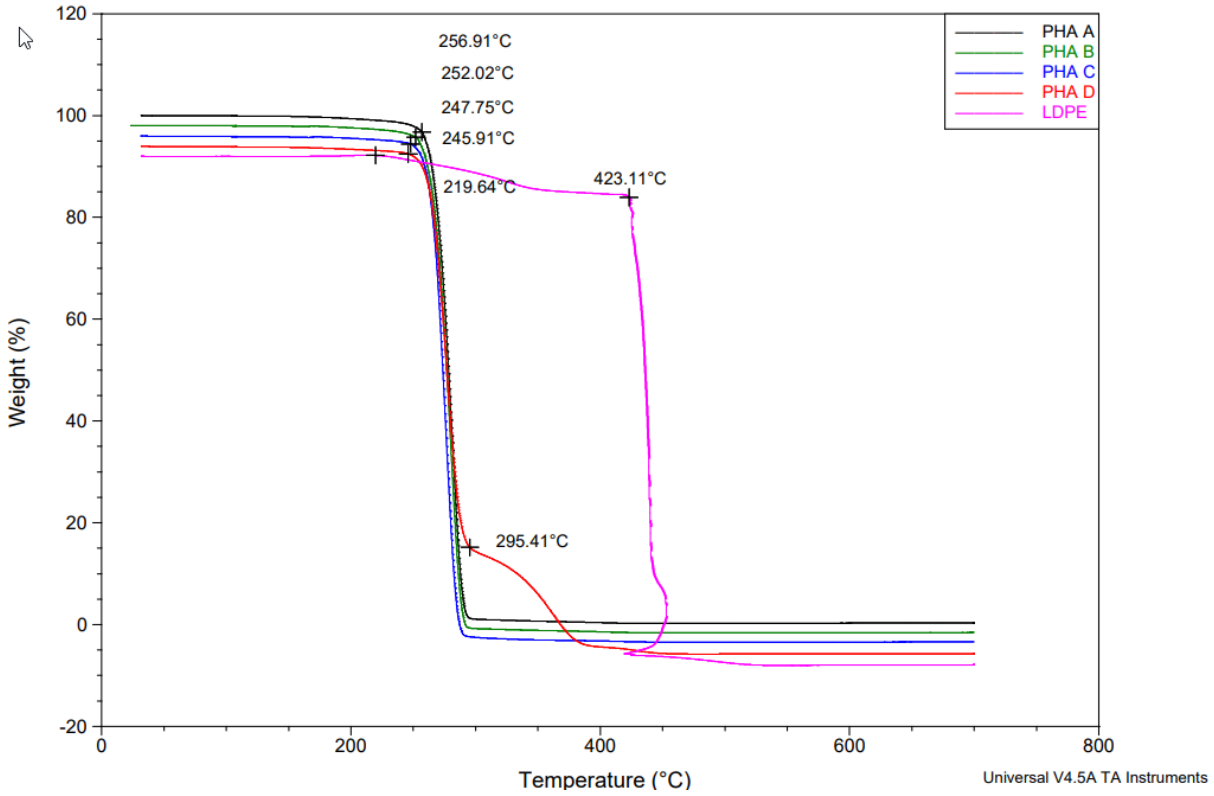

Figure 3.3: TGA results for the different PHAs studies and LDPE. (Note: The Y-axis of the TGA curves were offset for better visibility of the different thermograms.)

From the figure above it can be seen that all PHA samples start to thermal degrade steeply at the temperature range 245-257°C. However, the onset of thermal decomposition starts already at around 190°C. At this temperature, PHA likely starts depolymerizing and slowly decomposing up to the point at which the decomposition is then very fast (245-257°C). LDPE, on the other hand, starts to slowly decompose at around 219°C and the pronounced degradation happens only at 423°C. This indicates that PHA is less thermally stable than LDPE, as already reported in the literature[23]. The thermogram of PHA D also showed a second smaller decomposition step at around 295°C (Figure3.3), likely attributed to the presence of PBS in this PHA blend. This is in tune with the literature, in which it is reported that PBS starts to degrade at around 300°C[24].

3.3 DMA

Since the glass transition temperature (T_g) could not be retrieved by DSC, DMA was also carried on all the PHA samples. The T_g is a very relevant parameter for amorphous and semi-crystalline polymers (which is the case of the PHAs studied) and provides information about the temperature at which the polymer changes from a glassy state to a flexible rubbery state. As explained in the experimental section, the T_g value was taken as the temperature at which the maximum Tan(δ) value is attained in the temperature vs Tan(δ) curve (Figure3.4). The value of δ was calculated as the ratio between G" and G'.

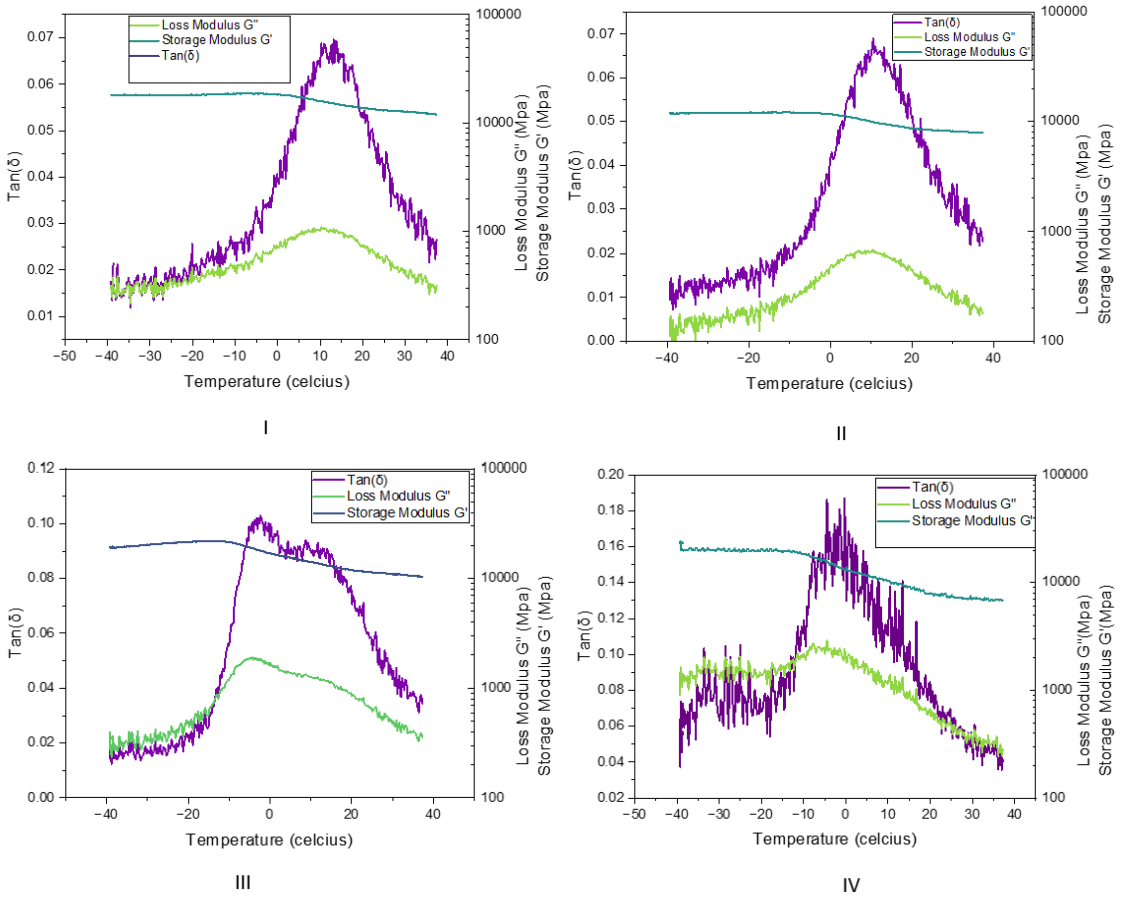

Figure 3.4: DMA curves for (I)PHA A, (II)PHA B, (III)PHA C, and (IV)PHA D

From the DMA curves above, one can observe that the Tan(δ) curve is very noisy for all the PHA samples. Thus, the estimated T_g values listed in Table:3.3 are only approximate. The reason for the noise, also observed for the G' and G" curves, could be related to the nature and physical stability of the PHA films, since these were rather thin(80-90μm).

Table 3.3: T_g values obtained in this study by DMA for all the PHA samples.

Material type	**T_g(°C)**
PHA A	12
PHA B	10
PHA C	-2
PHA D	-4

The T_g values obtained for PHA C and PHA D are similar to those reported in the respective technical data sheets, which were measured using DSC. However, for PHA A and PHA B, much higher T_g values were obtained by DMA in this study, compared to those reported in the technical data sheets using DSC. The reason for this significant difference is not well understood, and more studies would need to be carried out to clarify this. Nonetheless, if one looks only at the T_g values obtained in this study, there seems to be a correlation between these and the M_w of the different PHA samples. Surprisingly, PHA with lower M_w (PHA A and PHA B) had higher T_g values, and PHA with higher M_w (PHA C and PHA D) had lower T_g values. These results contradict the established overall qualitative dependence of T_g on M_w, in which T_g is expected to increase with increasing M_w. On the other hand, the results correlate with the fact that typically higher degree of crystallinity of the polymer (lower amount of amorphous regions) leads to increased T_g. This then indicates that for PHA materials, the degree of crystallinity has a stronger effect on T_g than M_w *per se*.

3.4 FTIR

FTIR spectroscopy was used to characterize the chemical composition of the different PHA samples. The obtained FTIR spectra can be seen in Figure3.5 below. All PHA samples presented similar FTIR spectra. The peak at 1719cm^{-1} is assigned to the presence of C=O vibration from the ester function in PHA. The peaks at 1179cm^{-1} and 1129cm^{-1}, represents C-O stretching and those at 1044cm^{-1} and, 979cm^{-1} are attributed to C-H bending vibration. The peak at 1274cm^{-1} may indicate the presence of amine moieties. Since PHA don't normally possess amine groups in their structure, this suggests the presence of amine-containing additives. Further studies would be required to find the type and exact composition of the additives but this was out of scope for this project.

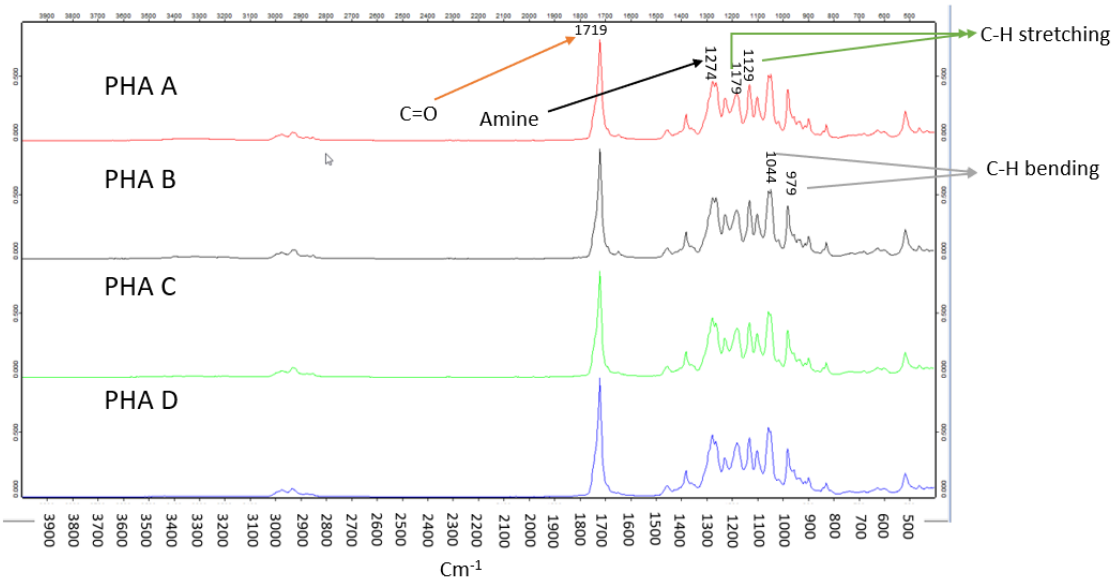

Figure 3.5: FTIR spectra PHA A(Red), PHA B(black), PHA C(green), PHA D(blue)

3.5 Mechanical properties

3.5.1 Tensile testing

Tensile testing was performed on films of all PHA types in order to determine the mechanical properties of the different materials. The results are summarized in the table below

Table 3.4: Summary of mechanical properties for all four PHA samples.

PHA Type	**Tensile stress(N/mm²)**	**Strain(%)**	**Young's Modulus(N/mm²)**
PHA A	32.4 ± 6.2	2.8 ± 0.1	11.7 ± 1.04
PHA B	33.3 ± 9.6	3.1 ± 0.2	11.0 ± 0.9
PHA C	20.6 ± 1.6	8.2 ± 7.3	3.6 ± 1.7
PHA D	20.5 ± 1.4	5.6 ± 0.7	3.6 ± 0.2

There are several factors that can affect the tensile strength (tensile stress) of polymers, namely temperature, strain rate, molecular weight, degree of crosslinking, and crystallinity[25]. Since all PHA samples were tested at the same environmental conditions (23°C and RH=50%) and strain rate, and there is no indication that the polymers are crosslinked, the discussion of mechanical properties will focus mainly on molecular weight and crystallinity. Tensile strength is expected to increase with increasing M_w since more entanglements can occur between the polymer chains and more force is needed to loosen up those entanglements[26] Surprisingly, the results show the opposite behaviour, i.e., PHA A and PHA B that have lower M_w than PHA C and PHA D (according to the respective technical data sheets), possessed

higher tensile strength. On the other hand, it is also known that tensile strength is expected to increase with increasing crystallinity, since the intermolecular bonding within the polymer chains increases[27]. The results show that PHA C and PHA D, which had the lowest crystallinity, were the ones presenting the lowest tensile strength, as would be expected. These results then indicate that, under the testing conditions used, the crystallinity of PHA had a stronger influence on the mechanical properties than Mw. Strain results also align with crystallinity results, i.e., PHA with higher crystallinity (PHA A and PHA B) deformed less before breaking (lower strain values). From the results, one can also conclude that the presence of PBS in PHA D didn't have a very big impact on the mechanical properties if one compares the strength and Elastic modulus values obtained for PHA C and PHA D, which have similar M_w according to the technical data sheets.

3.5.2 Heat sealing

In order to understand the optimal conditions to heat-seal the PHA films produced in-house and to analyze how strong the ensuing seals were, a heat-sealing test was performed at different temperatures (pressure and dwell time were kept constant), which was then followed by heat seal strength test. With this sequence of tests, it was not only possible to understand the influence of temperature on sealing, but also the maximum force the ensuring seals could withstand. The graphs in the image below show how the different temperatures used for heat sealing affected the strength of the formed seals for the different PHA films produced.

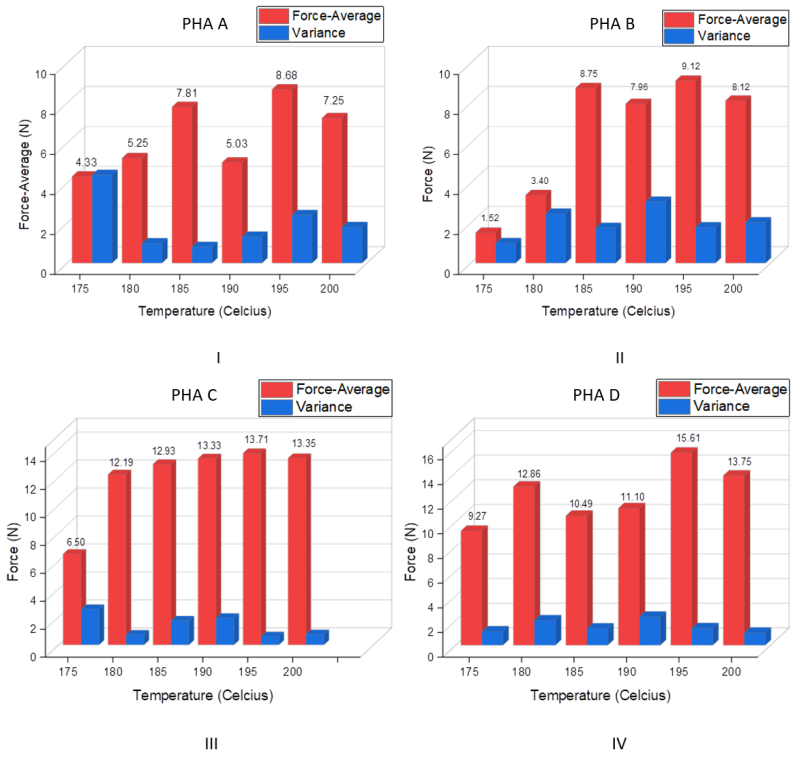

Figure 3.6: Seal strength of (I)PHA A, (II)PHA B, (III)PHA C and (IV)PHA D hot-pressed films at varying temperatures

The results show that the temperature really had an impact on the strength of the formed seals,i.e., on the force required to break the seals. For PHA C it is possible to observe that increasing temperature up to 195°C led to increased seal strength. This trend was not so evident for the other PHA samples, for which the seal strength varied randomly with changes in temperature. However, all PHA samples obtained the highest seal strength at 195°C, which indicates that this was the most adequate temperature to heat seal PHA samples. This temperature is 42-77°C higher than the T_m of the different PHA samples, thus the PHA samples were likely fully melted during heat-sealing. The absence of a clear relationship between temperature and force required to break the seal (i.e., seal strength) for PHA A, PHA B, and PHA D, may be related to the big variation in film thickness(60 - 90μm) for these samples (much more than for PHA C films). It is known that for thicker samples, at the same heat-sealing temperature, the strength required to break the seal increases[28]. Thus if some films of the same PHA type were thicker than others, it also influenced the seal strength results. Above 195°C, as indicated by TGA results, PHA starts to thermally decompose. Thus, the seal strength decreased for all PHA samples at 200°C, even if the dwell time used to heat-seal the samples was only 1 second.

Interestingly, there seems to be a good correlation between seal strength and crystallinity of PHA. Considering the maximum seal strength at 195°C, it is possible to observe that seal strength increased with decreasing PHA crystallinity in the order: PHA A (8.7N) < PHA B (9.1N) < PHA C (13.7N) < PHA D (15.6N). It is known that the seal initiation of semi-crystalline polymers, like the different PHA materials in this study, occurs when the amorphous fraction increases by heating, as the crystalline regions start disassembling and the polymer chains become more mobile[29]. Thus, under the heat-sealing conditions used in this study, i.e., for a short dwell time of 1 second, it was easier for the samples with lower crystallinity (meaning a bigger fraction of amorphous regions) to fully fuse and create a good seal. Also there seems to be a good correlation between seal strength and M_w at 195°C, and seal strength seems to increase with increasing M^w: PHA A (8.7N) < PHA B (9.1N) < PHA C (13.7N) < PHA D (15.6N).

3.6 Rheological properties

The rheology measurements are important for creating and preventing coating flaws on the paperboard. The measurements of interest in this thesis were,

- Melt viscosity
- Extensional viscosity
- Strain sweep test
- Frequency sweep test

These tests can show how the polymer melt behaves and how they behave when exposed to higher shear rates at the processing conditions.

3.6.1 Thermal stability of PHA

As mentioned above, PHAs can degrade when exposed to high temperatures(which are below those of the thermal decomposition of conventional fossil-based polymers). Thus, when exposed to high temperatures, some PHA polymers can show a drop in viscosity, which interferes with the change in viscosity upon increasing shear rate, and this can provide the wrong value of melt viscosity[24]. So it is primarily necessary to determine the safe operating temperature for measuring the rheological properties.

To assess the thermal degradation of the polymer, the loss modulus(G") and storage modulus(G') are measured with respect to a constant amplitude of 0.05 and frequency of 1Hz. For reference, the same measurement is also done for LDPE.

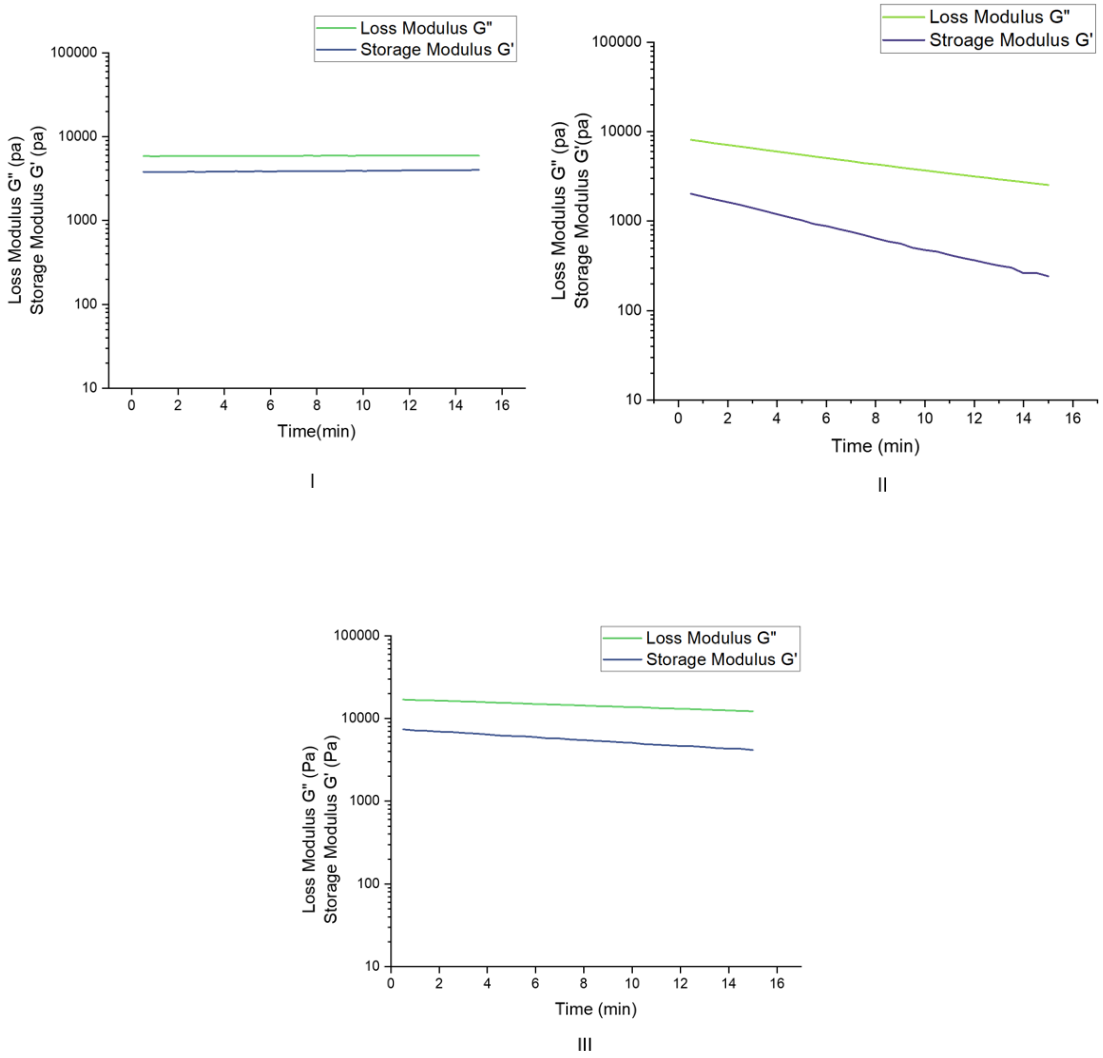

Figure 3.7: Thermal stability of the (I)LDPE 175 at °C, (II)PHA A at 175°C,and (III)PHA A at 160°C

From the figure above, one can see that the G' and G" lines for LDPE are straight which indicates that the material is stable at 175°. However, for PHA A, one can

see that, the G' and G" lines create a declining slope with increasing time. This indicates that the material starts to degrade with time at temperatures above its melting point, likely due to a decrease in molecular weight. The slope is steeper for PHA A at 175°C which was the material preparation temperature and pilot plant processing temperature. However, the degradation process seems to be slower for PHA A at 160°C. This phenomenon is observed for other PHA samples as well FigureA.4. To weaken the influence of thermal degradation on rheological data, the measurement temperatures were kept at 160°C.

3.6.2 Relaxation behaviour of PHA

The linear viscoelastic region of the polymer amplitude sweep was assessed with a constant frequency of 1Hz. The amplitude sweep provides the limit of the linear viscoelastic region and the range in which the frequency sweep test can be operated. The images below represent the amplitude sweep test of LDPE and PHA's.

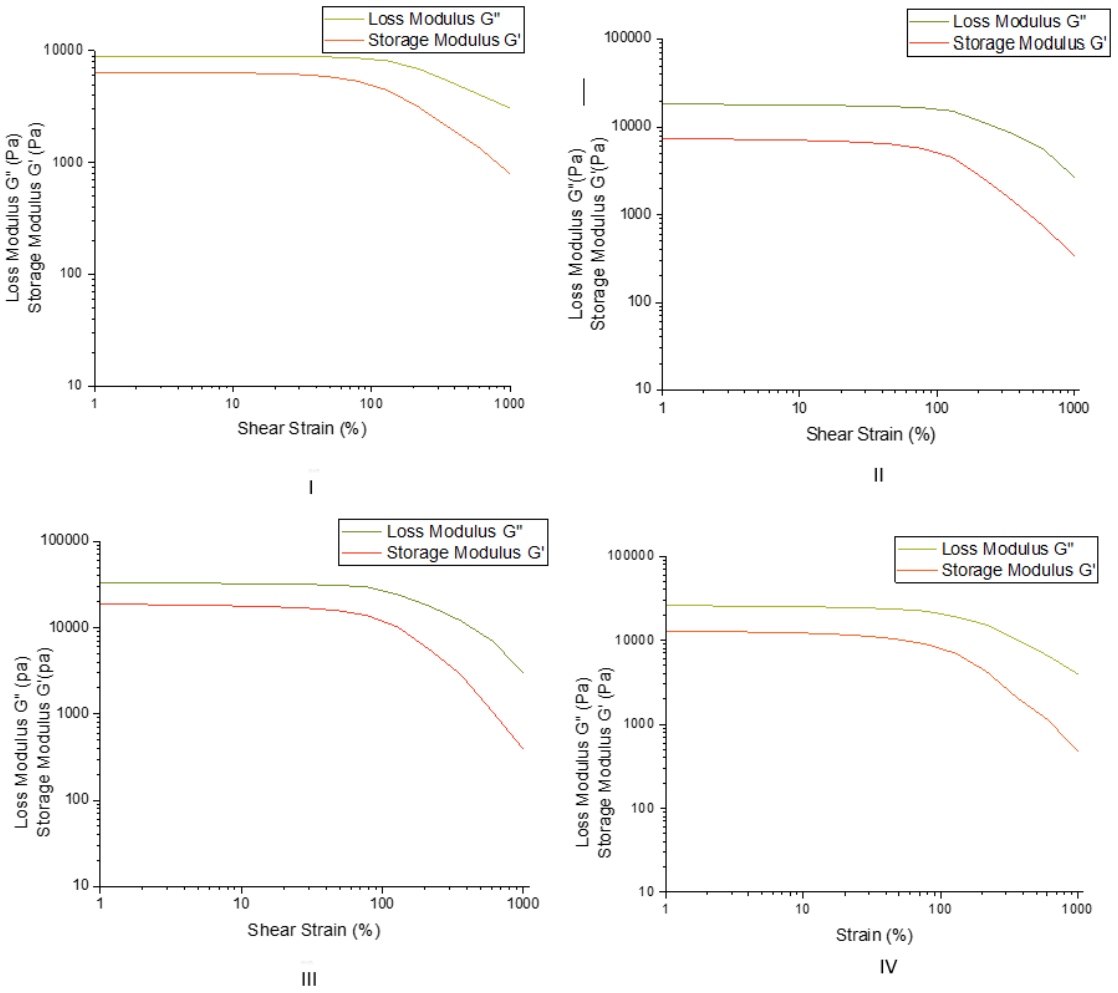

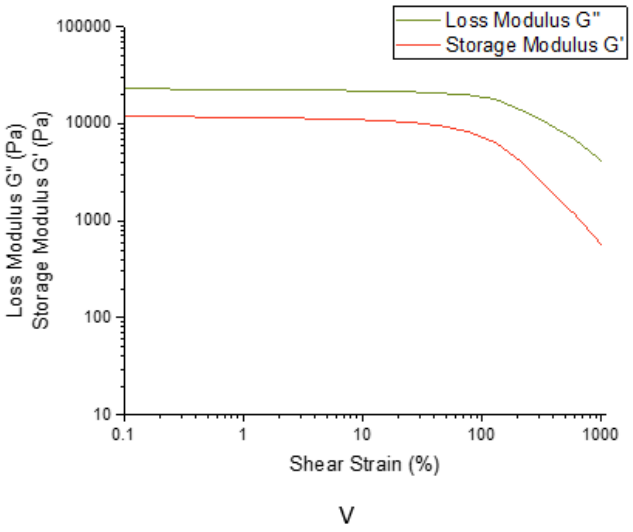

Figure 3.8: Amplitude sweep graph for (I)LDPE, (II)PHA A, (III)PHA B, (IV)PHA C, and (V)PHA D

The graphs in Figures3.8 indicate that G' lines are horizontally straight for all PHA's and LDPE at frequency range 0.1Hz to 10Hz. This indicates the linear viscoelastic region of these polymers, and from this, a constant frequency of 1Hz was taken for the frequency sweep test. Apart from this, it was possible to observe that at any given point in the viscoelastic region the value of G" is greater than G', which indicates that all the samples showed fluid structure and behave as viscoelastic fluid.

The frequency sweep test is also useful to obtain more characteristic information about polymer melt. The viscoelastic properties of the polymer may change over time and these oscillation measurements can be useful to determine their long-time behaviour. Figure3.9 shows the cross-over of G" and G' along with phase angles.

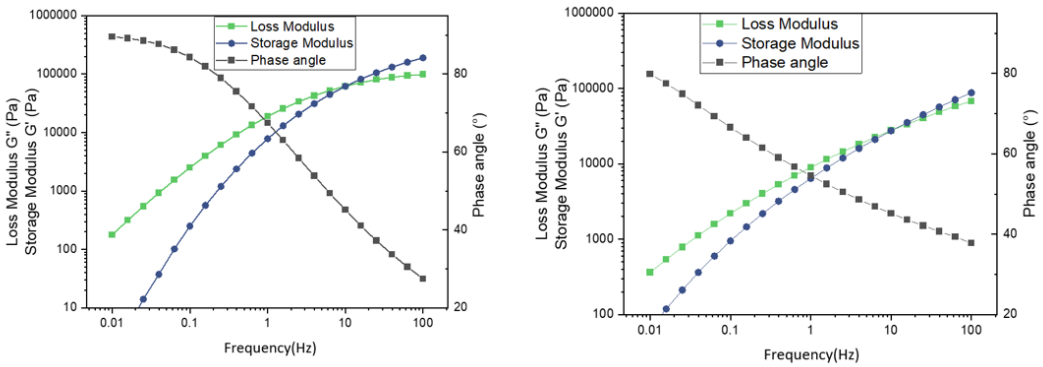

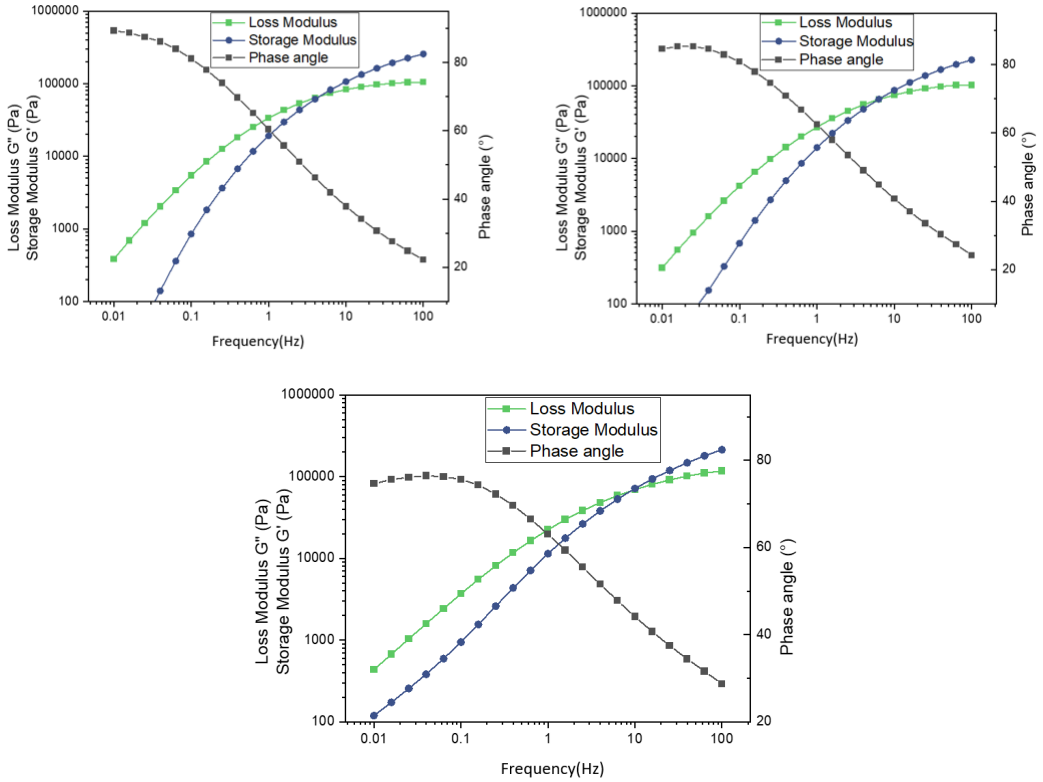

Figure 3.9: Frequency sweep graph (I)LDPE, (II)PHA A, (III)PHA B, (IV)PHA C, (V)PHA D

The crossover point indicates the phase transition of the material and it shows the time taken by each material to change from elastic material(before cross-over frequency) to viscous material(after cross-over frequency). The table below summarizes the cross-over frequencies.

Table 3.5: Cross over frequencies for LDPE and different PHAs studied

Material type	**Cross over frequency(Hz)**	G"**(Pa)**	G'**(Pa)**
LDPE	0.1	27463	27651
PHA A	0.1	61739	61993
PHA B	0.25	61201	63983
PHA C	0.15	65020	65020
PHA D	0.1	69582	71704

The cross-over frequency values in the table above indicate that for lower and higher molecular weight PHA's the time taken to change into viscous behaviour is the same as that for LDPE. The graph in the image above also indicates the Phase angle(δ) for LDPE and PHAs. The Phase angle is a relative measure of the material's viscous and elastic properties. For LDPE and PHAs, it is possible to observe that at lower frequencies the phase angle is almost 90° indicating that these materials are of a viscous nature. Therefore they do not possess a yield stress.

3.6.3 Frequency sweep test and Non-Newtonian behaviour

In the frequency sweep test, the complex viscosity was measured over a range of frequencies. The frequency sweep graph is shown in the image below. It is possible to observe that there are two complex viscosities lines for each PHA. The complex viscosity indicates the frequency sweep from 100Hz to 0.01Hz and the complex viscosity reverse indicates the frequency sweep from 0.01Hz to 100Hz

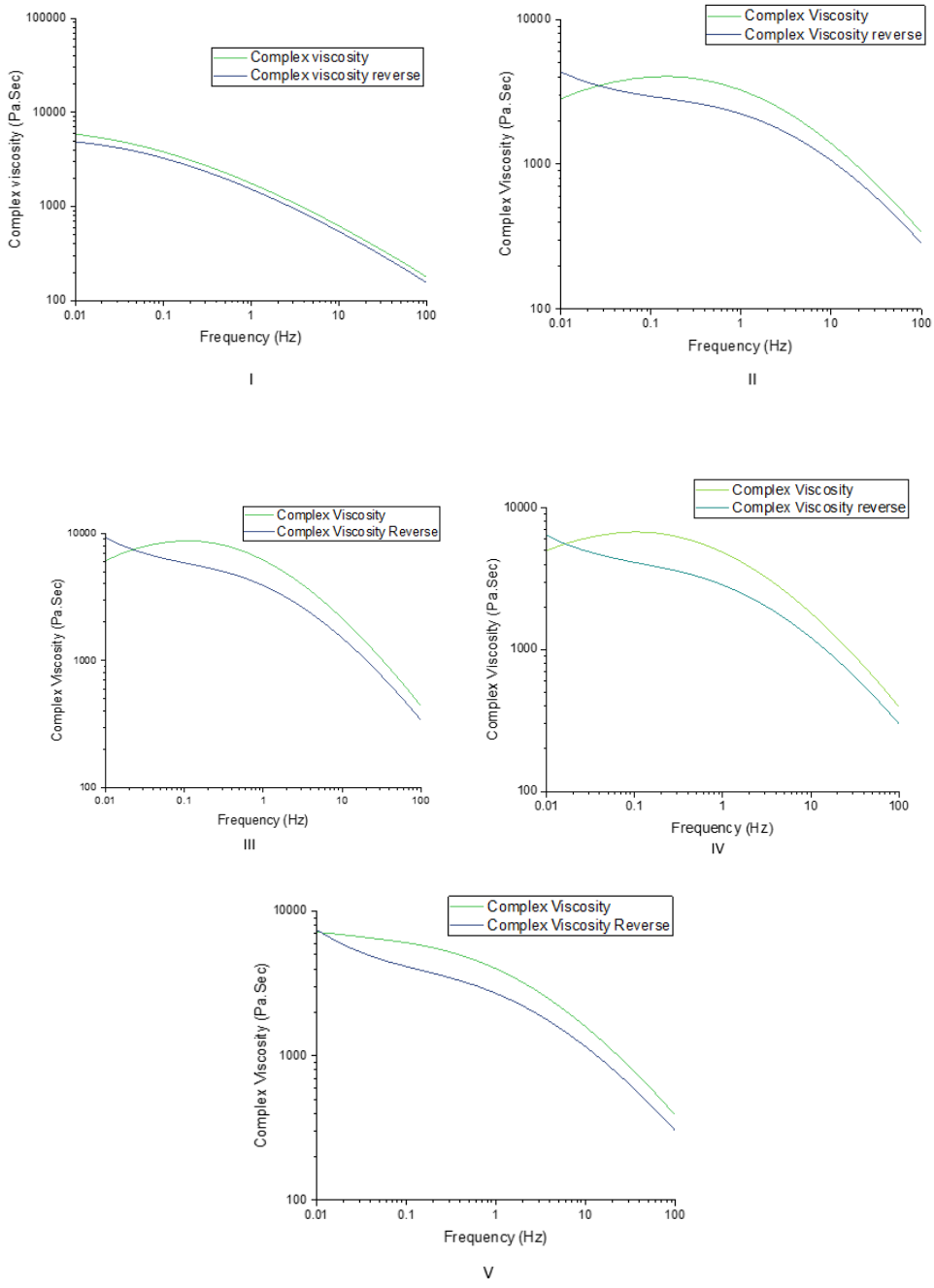

Figure 3.10: Complex viscosity graphs for (I)LDPE, (II)PHA A, (III)PHA B, (IV)PHA C, (V)PHA D

From Figure:3.10, it is observed that both viscosity curves showed the same path for LDPE. However, this was not the case for the PHAs. For PHAs, from the intermediate to high-frequency range(0.1Hz to 100Hz), all showed shear thinning behaviour, proving the polymer melt is a Non-Newtonian fluid. From low to intermediate frequency range(0.01Hz to 0.1Hz), there is a sudden drop in viscosity in the complex curves except for PHA D. The sudden drop in viscosity might be attributed to the thermal degradation of the polymer. For PHA D alone, the complex viscosity is the same for both viscosity curves. This indicates that the blending with PBS may have improved the thermal stability of this PHA. Another reason for the increase in stability could be the monomer ratio, as different PHAs have different monomer ratios.

3.6.4 Melt Viscosity

The melt viscosities were measured with a capillary rheometer. As mentioned earlier, capillary rheometers were used to measure melt viscosity at process-relevant shear rates. The melt viscosities were measured by going from higher shear rates to lower shear rates.

The image below represents the corrected melt viscosities of LDPE and of all four PHA studied. From this image, it is possible to observe that with an increase in shear rate, the melt viscosities decreases, which indicates the polymer melt has shear thinning behaviour, even at higher shear rates. The line of viscosity s almost straight for LDPE. However, for PHAs the viscosity lines have more fluctuations. These fluctuations indicate that PHAs are pressure-sensitive materials. Among the PHAs studied, the line of PHA D is a close resemblance to that of LDPE, which suggests that with an increase in the molecular weight and blending with other polymers(in this case PBS), the material stability can also be increased.

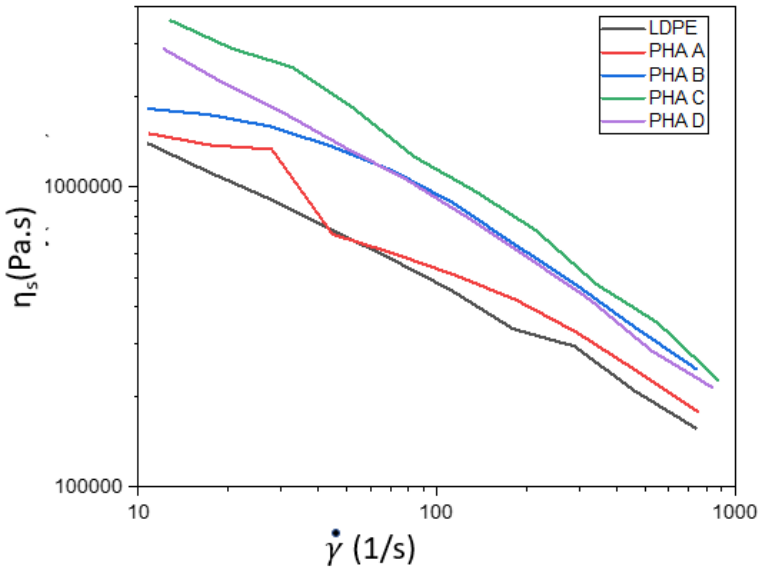

Figure 3.11: Melt viscosities for LDPE and PHA studied

3.7 WVTR

The water vapour transmission rate of all PHA films and some of the PHA-coated paperboards (with PHA A, PHA C, and PHA D) was assessed at two different environmental conditions: normal (23°C and RH=50%) and tropical (38°C and RH=80%). From Figure3.12, it is observed that all samples presented higher WVTR values than the reference sample (LDPE) in all conditions. This shows that PHA materials still require some developments in order to attain as good water vapor barrier performance as LDPE-based materials.

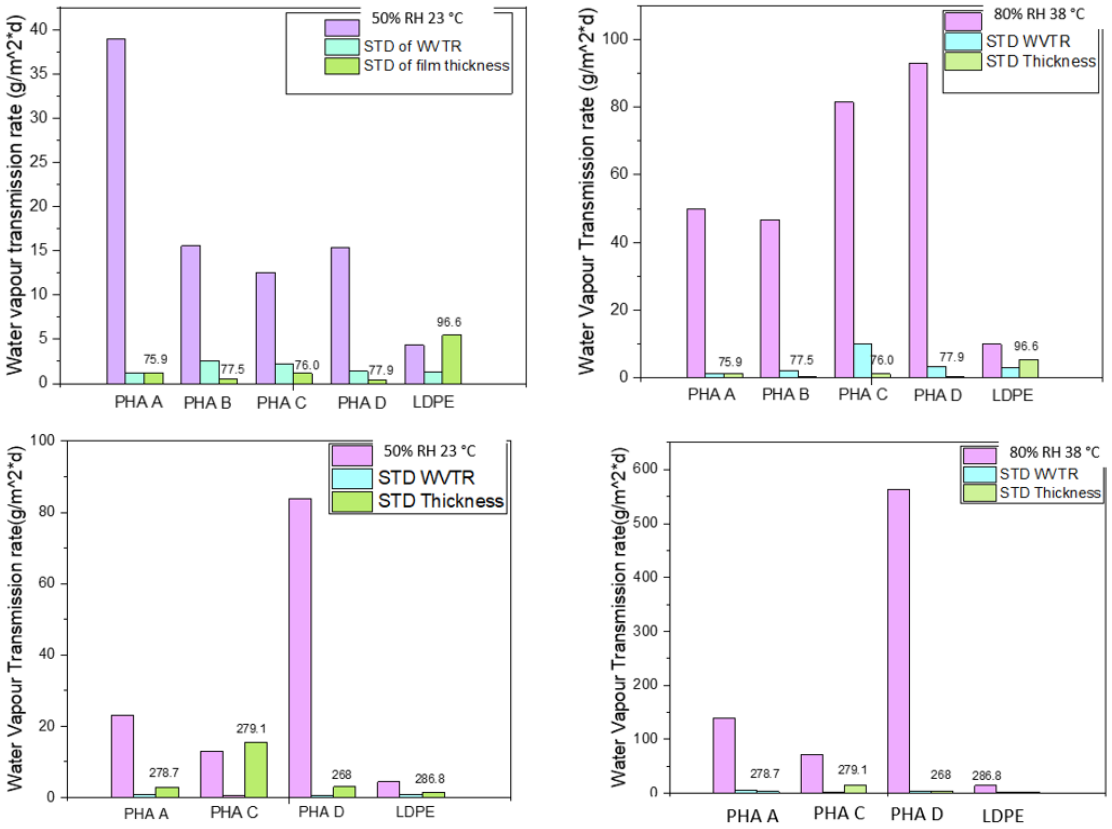

Figure 3.12: WVTR results of PHA films (top) and PHA-coated paperboards (bottom) at normal (left) and tropical conditions (right).

At normal conditions, PHA C (both in the form of film and coated paperboard) showed the lowest WVTR values. Nonetheless, it is worth noting that samples containing PHA C were the ones possessing high variation in film/coating thickness. Interestingly, in tropical conditions, the paperboard coated with PHA C still presented the lowest WVTR value, but not the PHA C film. Instead, at these conditions, PHA B film was the one presenting the lowest WVTR value, which was close to that of PHA A film.

If one only looks at the WVTR results obtained for the PHA films (Figures3.12 top), it seems that at normal conditions (lower relative humidity – RH=50%), M_w of PHA played a bigger role than PHA crystallinity, in the sense that PHA C

and PHA D were the samples presenting the lowest values. Conversely, at tropical conditions (higher relative humidity – RH=80%), the crystallinity of PHA seems to have had a stronger effect than M_w of PHA, as PHA A and PHA B were the ones with lower WVTR values. Figure3.13 also corroborates this conclusion. Whereas at normal conditions there seems not to be any correlation between WVTR values and degree of crystallinity (R^2=0.3), At tropical conditions one can see a good correlation between these two parameters and a trendline with R^2=0.93 can be obtained.

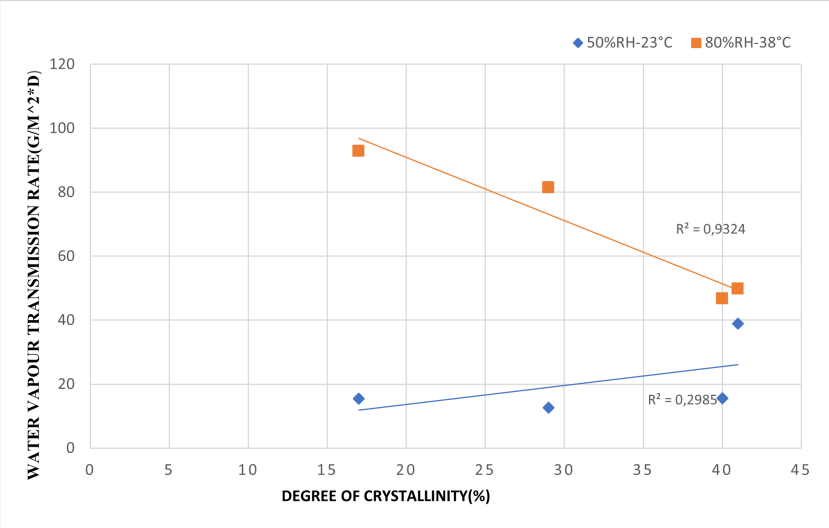

Figure 3.13: WVTR *vs* degree of crystallinity of PHA at normal(blue) and tropical conditions(orange)

For PHA-coated paperboards, the WVTR values under both normal and tropical conditions increased in the order PHA C< PHA A< PHA D. The reason for this behavior is not well understood and more studies would be required to draw any good conclusions. It is still worth noting that when it comes to extrusion-coated paperboards, factors other than the PHA characteristics start playing an important role in water vapor barrier performance, including film homogeneity, edge stability, pinholes, etc.

4
Conclusion and Future work

4.1 Conclusion

In this project four different PHA types were evaluated. The melting temperature, glass transition temperature, and degradation temperature were determined to better understand the thermal behavior of the materials and try to improve their processing conditions. From the DSC and DMA analysis, it was found that increased molecular weight of PHA generally led to increased melting temperature and decreased glass transition temperature. TGA analysis showed that the PHA polymers start decomposing already at temperatures around 190°C, so temperatures lower (or at least not much higher) than 190°C would be recommended for real-life processing.

PHA crystallinity also seems to play an important role both in tensile strength and heat-seal strength of PHA materials; tensile strength seems to increase with increasing crystallinity, whereas heat-seal strength seems to increase with decreasing crystallinity (and increasing M_w). The highest heat seal strength for all four PHA types was obtained at 195°C, and above this temperature the strength started to decrease, likely due to thermal decomposition.

The rheological studies showed that PHAs are not thermally stable at high temperatures, and the time period that a material is exposed to high temperatures is of importance. The rheological studies also showed that with a higher shear rate, the material showed shear thinning fluid behavior and no yield stress, which makes it easier to coat on paperboard. However, for the high molecular weight PHAs, coating can be more difficult as the melt viscosities are also higher.
Finally, the WVTR of the different PHA samples was evaluated to assess their water vapor barrier performance. It was shown that both molecular weight and crystallinity of the polymer play an important role when it comes to WVTR but at different environmental conditions. The former plays a bigger role at normal conditions (23°C and RH=50%), whereas the latter plays a more significant role at tropical conditions (38°C and RH=80%).

4.2 Future work

Some future work could include
• Measuring the M_w values of PHAs.

• Measuring the melt flow index of the polymers to obtain more information on the flow of the polymer on the paperboard.

• Testing the grease barrier performance against different types of food products such as mayonnaise, oil, chicken fat *etc.*

• Testing the swelling of the PHA materials when exposed to water.

References

[1] Yuanfeng Pan, Madjid Farmahini-Farahani, Perry O'Hearn, Huining Xiao, and Helen Ocampo. An overview of bio-based polymers for packaging materials. *J. Bioresour. Bioprod*, 1(3):106–113, 2016.

[2] Marina Ramos, Arantzazu Valdés, Ana Cristina Mellinas, and María Carmen Garrigós. New trends in beverage packaging systems: A review. *Beverages*, 1(4):248–272, 2015.

[3] Katarzyna Leja and Grażyna Lewandowicz. Polymer biodegradation and biodegradable polymers-a review. *Polish Journal of Environmental Studies*, 19(2), 2010.

[4] Karoliina Emilia Helanto, Lauri Matikainen, Riku Talja, and Orlando J Rojas. Bio-based polymers for sustainable packaging and biobarriers: A critical review. *BioResources*, 14(2):4902–4951, 2019.

[5] Yuanfeng Pan, Madjid Farmahini-Farahani, Perry O'Hearn, Huining Xiao, and Helen Ocampo. An overview of bio-based polymers for packaging materials. *J. Bioresour. Bioprod*, 1(3):106–113, 2016.

[6] José GB Derraik. The pollution of the marine environment by plastic debris: a review. *Marine pollution bulletin*, 44(9):842–852, 2002.

[7] Alistair J Anderson and EA372789 Dawes. Occurrence, metabolism, metabolic role, and industrial uses of bacterial polyhydroxyalkanoates. *Microbiological reviews*, 54(4):450–472, 1990.

[8] Aamer Ali Shah, Fariha Hasan, Abdul Hameed, and Safia Ahmed. Biological degradation of plastics: a comprehensive review. *Biotechnology advances*, 26(3):246–265, 2008.

[9] Jingnan Lu, Ryan C Tappel, and Christopher T Nomura. Mini-review: biosynthesis of poly (hydroxyalkanoates). *Journal of Macromolecular Science®, Part C: Polymer Reviews*, 49(3):226–248, 2009.

[10] Siddharth Priyadarshi, A Shukla, and B Bhaskarrao-Borse. Polyhydroxyalkanoates: role of ralstonia eutropha. *International Journal of Biomedical And Advance Research*, 5(02), 2014.

[11] Elodie Bugnicourt, Patrizia Cinelli, Andrea Lazzeri, and Vera Alejandra Alvarez. Polyhydroxyalkanoate (pha): Review of synthesis, characteristics, processing and potential applications in packaging. 2014.

[12] CSK Reddy, Rashmi Ghai, V_C Kalia, et al. Polyhydroxyalkanoates: an overview. *Bioresource technology*, 87(2):137–146, 2003.

[13] Hajime Nakajima, Peter Dijkstra, and Katja Loos. The recent developments in biobased polymers toward general and engineering applications: Polymers that

are upgraded from biodegradable polymers, analogous to petroleum-derived polymers, and newly developed. *Polymers*, 9(10):523, 2017.

[14] Celia Somlai, Craig Bullock, and John Gallagher. Plastic packaging waste in europe: Addressing methodological challenges in recording and reporting. *Waste Management & Research*, page 0734242X221142192, 2023.

[15] Carolina E Realini and Begonya Marcos. Active and intelligent packaging systems for a modern society. *Meat science*, 98(3):404–419, 2014.

[16] Bertram Hubert Gregory. *Extrusion Coating: A Process Manual*. Trafford Publishing, 2005.

[17] Joseph D Menczel, Lawrence Judovits, R Bruce Prime, Harvey E Bair, Mike Reading, and Steven Swier. *Differential scanning calorimetry (DSC)*, volume 7. Wiley, Hoboken, NJ, 2009.

[18] Jisuk Lee, Yuta Hikima, Takafumi Sekiguchi, and Masahiro Ohshima. Thermal, rheological, and mechanical properties of cellulose nanofiber (cnf) and poly (3-hydroxybutyrate-co-3-hydroxyhexanoate)(phbh) biopolymer nanocomposites. *Cellulose*, 29(7):3901–3913, 2022.

[19] Richard P Chartoff, Joseph D Menczel, and Steven H Dillman. Dynamic mechanical analysis (dma). *Thermal analysis of polymers: fundamentals and applications*, 387, 2009.

[20] R Bruce Prime, Harvey E Bair, Sergey Vyazovkin, Patrick K Gallagher, and Alan Riga. Thermogravimetric analysis (tga). *Thermal analysis of polymers: Fundamentals and applications*, pages 241–317, 2009.

[21] Shuyi Wu, Yang Zhang, Jiarui Han, Zhining Xie, Jun Xu, and Baohua Guo. Copolymerization with polyether segments improves the mechanical properties of biodegradable polyesters. *ACS omega*, 2(6):2639–2648, 2017.

[22] María Jordá-Reolid, Ana Ibáñez-García, Linda Catani, and Asunción Martínez-García. Development of blends to improve flexibility of biodegradable polymers. *Polymers*, 14(23):5223, 2022.

[23] Ashutosh Kr Chaudhary, Shubham P Chitriv, Kundrapu Chaitanya, and RP Vijayakumar. Influence of ultraviolet and chemical treatment on the biodegradation of low-density polyethylene and high-density polyethylene by cephalosporium strain. *Environmental Monitoring and Assessment*, 195(3):395, 2023.

[24] Qi Liao, Isao Noda, and Curtis W Frank. Melt viscoelasticity of biodegradable poly (3-hydroxybutyrate-co-3-hydroxyhexanoate) copolymers. *Polymer*, 50(25):6139–6148, 2009.

[25] Mohammad Amjadi and Ali Fatemi. Tensile behavior of high-density polyethylene including the effects of processing technique, thickness, temperature, and strain rate. *Polymers*, 12(9):1857, 2020.

[26] Joseph Aliyu. How molecular weight affects mechanical properties of polymers? 10 2018.

[27] Christopher Dartiailh, Warren Blunt, Parveen K Sharma, Song Liu, Nazim Cicek, and David B Levin. The thermal and mechanical properties of medium chain-length polyhydroxyalkanoates produced by pseudomonas putida ls46 on various substrates. *Frontiers in Bioengineering and Biotechnology*, 8:617489, 2021.

[28] Ilknur Ilhan, Deniz Turan, Ian Gibson, and Roland ten Klooster. Understanding the factors affecting the seal integrity in heat sealed flexible food packages: A review. *Packaging technology and science*, 34(6):321–337, 2021.

[29] Bram Bamps, Mieke Buntinx, and Roos Peeters. Seal materials in flexible plastic food packaging: A review. *Packaging Technology and Science*, 2023.

A

Appendix 1

A.1 DSC

The below pictures shows the DSC graph of other PHA's.

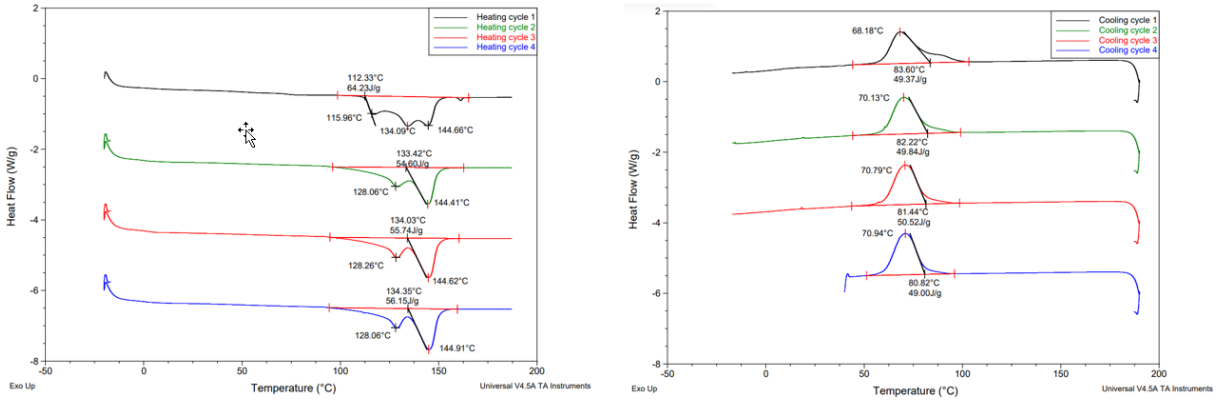

I II

Figure A.1: DSC graph of PHA B (I). Heating cycles (II). Cooling cycles

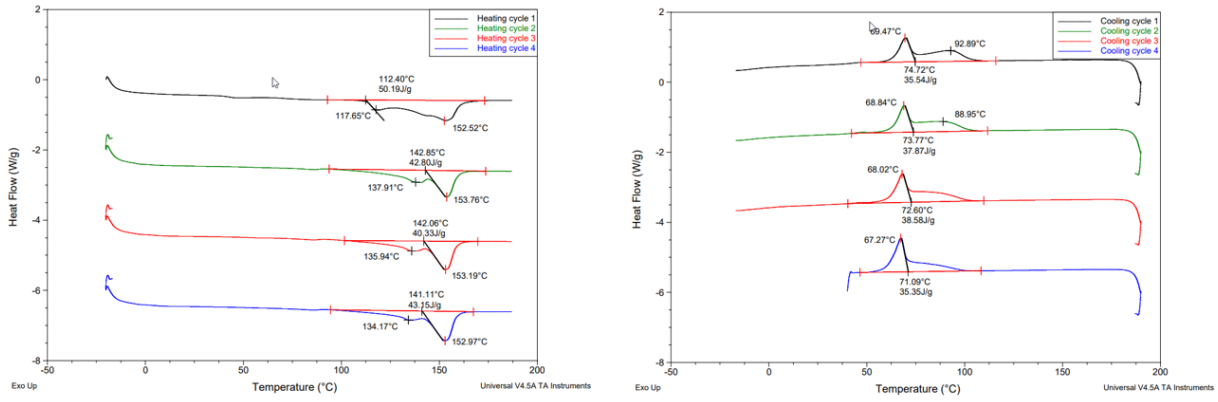

I II

Figure A.2: DSC graph of PHA C (I). Heating cycles (II). Cooling cycles

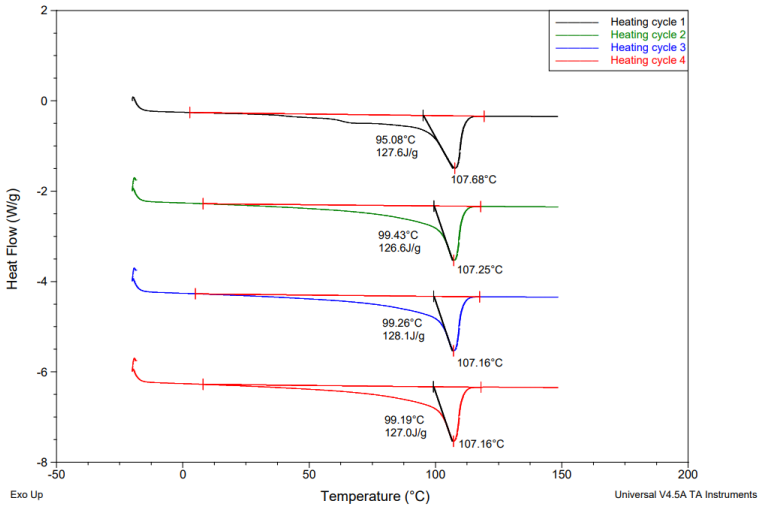

Figure A.3: DSC graph of LDPE

A.2 Rheological properties

A.2.1 Thermal stability of PHA

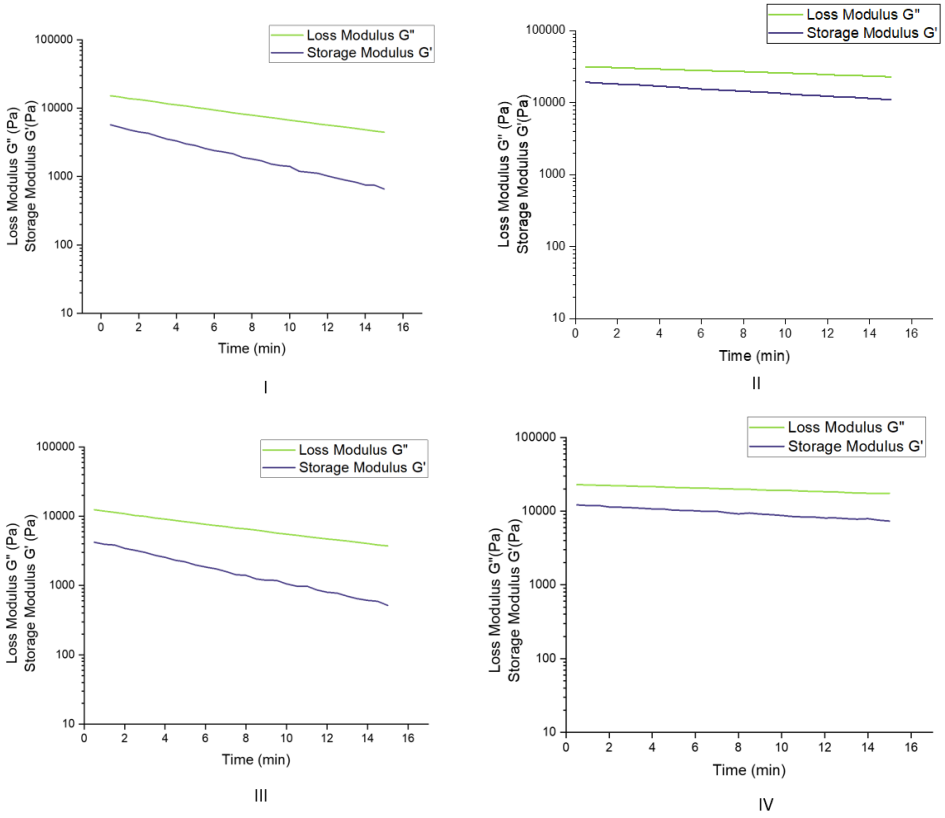

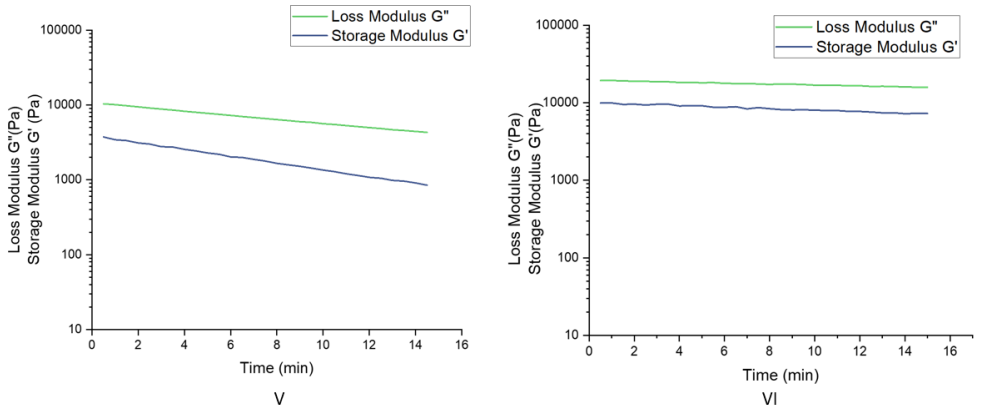

Figure A.4: Thermal stability of PHA's (I)PHA B at 175°C, (II)PHA B at 160°C, (III)PHA C at 175°C, (IV)PHA C at 160°C, (V)PHA D at 175°C, (VI)PHA D at 160°C

A.3 Mechanical properties

A.3.1 Heat sealing test

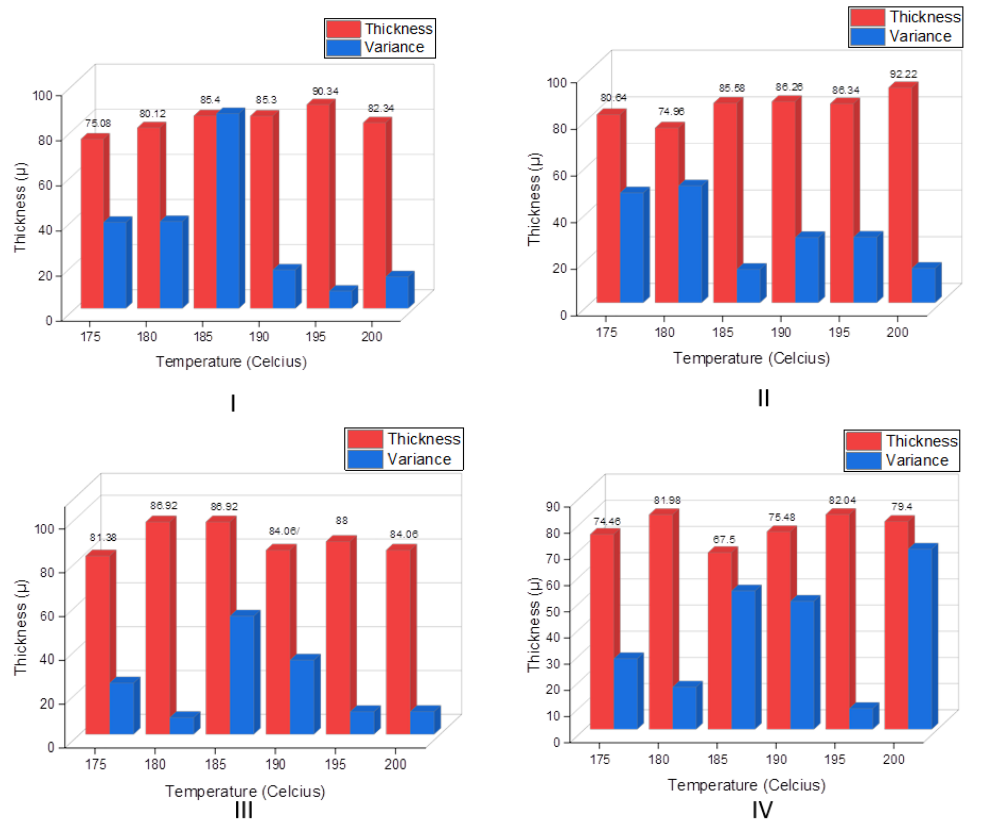

Figure A.5: Thickness variation of the film used for heat sealing (I)PHA A, (II)PHA B, (III)PHA C, (IV)PHA D

DEPARTMENT OF INDUSTRIAL AND MATERIAL SCIENCE
CHALMERS UNIVERSITY OF TECHNOLOGY
Gothenburg, Sweden
www.chalmers.se

CHALMERS
UNIVERSITY OF TECHNOLOGY